

Research Article

Designing a Novel Aerolysin-based Multiepitope Vaccine against *Aeromonas hydrophila* Isolated from *Osphronemus goramy* Using Reverse Vaccinology: An In Silico Approach

Rozi^{1,7}, Wiwiek Tyasningsih², Jola Rahmahani², Eduardus Bimo Aksono³, Muchammad Yunus⁴, Mohammad Anam Al Arif⁵, Suryo Kuncorojati⁶, Rahayu Kusdarwati⁷, Putri Desi Wulan Sari⁷, Mohammad Noor Amal Azmai⁸, Annas Salleh⁹, Nadeem Khanand¹⁰, and Suwarno²

¹Doctoral Program of Veterinary Science, Faculty of Veterinary Medicine, Universitas Airlangga, Surabaya 60115. Indonesia

²Division of Microbiology, Faculty of Veterinary Medicine, Airlangga University, Surabaya 60115. Indonesia

³Division of Basic Veterinary Medicine, Faculty of Veterinary Medicine, Airlangga University, Surabaya 60115. Indonesia

⁴Division of Veterinary Parasitology, Faculty of Veterinary Medicine, Airlangga University, Surabaya 60115. Indonesia

⁵Division of Farm, Faculty of Veterinary Medicine, Airlangga University, Surabaya 60115. Indonesia

⁶Division of Veterinary Anatomy, Faculty of Veterinary Medicine, Airlangga University, Surabaya 60115. Indonesia

⁷Department of Aquaculture, Faculty of Fisheries and Marine, Airlangga University, Surabaya 60115. Indonesia

⁸Department of Biology, Faculty of Science, Universiti Putra Malaysia. Malaysia

⁹Department of Veterinary Laboratory Diagnosis, Faculty of Veterinary Medicine, Universiti Putra Malaysia. Malaysia

¹⁰Department of Bioinformatics, School of Interdisciplinary Engineering and Sciences, National University of Science and Technology, Islamabad. Pakistan.



ARTICLE INFO

Received: August 24, 2024

Accepted: Sept 22, 2024

Published: Oct 01, 2024

Available online: Oct 23, 2024

*) Corresponding author:

E-mail: suwarno@fkh.unair.ac.id

Keywords:

Immunoinformatics

Multi-epitopes vaccine

Molecular Docking

A. hydrophila



This is an open access article under the CC BY-NC-SA license (<https://creativecommons.org/licenses/by-nc-sa/4.0/>)

Abstract

Aeromonas hydrophila, a gram-negative bacterium, is a major pathogen responsible for various diseases in mammals, reptiles, amphibians, fish, and humans. Targeting the specific toxin aerolysin in *A. hydrophila* is crucial to address antibiotic resistance and the lack of adequate and protective vaccines against this intracellular and extracellular pathogen. This study aimed to identify a multi-epitope vaccine (MEV) candidate targeting the aerolysin toxin to combat the disease effectively. Standard biochemical characterization methods, detection of PCR, and sequencing of the 16S rRNA, rpoB, and aerA genes identified the isolate AHSA1 as *A. hydrophila* isolated from *O. goramy*. Subsequently, we identified B and T cell epitopes on the aerolysin protein and predicted MHC-I and MHC-II epitopes. The epitopes were then evaluated for toxicity, antigenicity, allergenicity, and solubility. The vaccine design integrated multi-epitope constructs, utilizing specialized linkers (GPGPG and EAAAK) to connect epitope peptides with the cholera toxin B subunit as an adjuvant, thereby enhancing immunogenicity. Ramachandran plots showed that 85.25% of the residues were in the most favorable regions, followed by additionally allowed regions (10.80%), generously allowed regions (1.30%), and disallowed regions (2.65%), confirming the feasibility of the modeled vaccine design. Based on docking simulations, the MEV had strong binding energies with TLR-4 (-1081.4 kcal/mol), TLR-9 (-723.2 kcal/mol), MHC-I (-866.2 kcal/mol), and MHC-II (-9043.3 kcal/mol). Based on computational modeling, we expect the aerolysin MEV candidate to activate diverse immune mechanisms, stimulate robust responses against *A. hydrophila*, and maintain safety. The significant solubility, absence of toxicity and allergic response contribute to the potential clinical utility of this vaccine candidate.

Cite this as: Rozi., Tyasningsih, W., Rahmahani, J., Aksono, E. B., Yunus, M., Al Arif, M. A., Kuncorojati, S., Kusdarwati, R., Sari, P. D. W., Azmai, M. N. A., Salleh, A., Nadeem Khanand, N., & Suwarno. (2024). Designing a Novel Aerolysin-based Multiepitope Vaccine against *Aeromonas hydrophila* Isolated from *Osphronemus goramy* Using Reverse Vaccinology: An In Silico Approach. *Jurnal Ilmiah Perikanan dan Kelautan*, 16(2):298–321. <https://doi.org/10.20473/jipk.v16i2.62035>

1. Introduction

Aeromonas hydrophila, a mesophilic, motile, Gram-negative bacterium with a short bacillus shape that produces oxidase and catalase enzymes, is a type of bacterium found in marine, brackish, and freshwater that can cause diseases in various animals like fish, amphibians, reptiles, birds, and mammals (Janda and Abbot, 2010; Pablos et al., 2011; Abdella et al., 2023). *Aeromonas* species can be found in various aquatic environments such as sediments, estuaries, seaweeds, seagrasses, water sources, and food (Vivekanandhan et al., 2002; Matyar et al., 2007; Martinez-Murcia et al., 2008). *Aeromonas* is responsible for various diseases in fish, including Motile Aeromonas Septicemia (MAS), Motile Aeromonas Infection (MAI), hemorrhagic conditions, ulcerative diseases, septicemia, furunculosis, and red wound disease (Albert et al., 2000; Abbott et al., 2003; Fang and Sin, 2004; Rozi et al., 2018a). Outbreaks of aeromonad motile septicemia are common worldwide and have been reported in various regions, including Australia, the southeastern states of America, Spain, and the Southeast Asian region (Pippy and Hare, 1969; Hofer et al., 2006; Xu, et al 2023). *Aeromonas* is a pathogen known to cause diseases in more than 20 different fish species, leading to significant economic losses in the aquaculture industry. It particularly affects carp, with annual losses estimated at around 2,200 tons (Nielsen et al., 2001; Zhang et al., 2002). Additionally, the Alabama Fish Farming Center reports losses of 10,500 tons, with vAh isolates representing 35% of disease cases (Pridgeon et al., 2014). Outbreaks of motile aeromonad septicemia typically occur when fish have weakened immunity due to overcrowding or other diseases (Pang et al., 2015; Xu., et al 2023).

A. hydrophila, a bacterium found in human feces, is a significant pathogen affecting aquaculture and human health (Pang et al., 2015; Dubey et al., 2022; Pessoa et al., 2022). It infects aquatic organisms and causes many infectious diseases in newborns and adults. The bacterium has been found in over 20 countries across six continents, with tropical and subtropical nations predominantly hosting *A. hydrophila* infections (Janda and Abbott, 2010; Nolla et al., 2017). Fish, the leading carriers of *Aeromonas*, have a significant role in transmitting diseases to humans through consumption, resulting in various health problems. It is responsible for a significant percentage of clinical isolations related to human illnesses, including gastroenteritis, septicemia, wound infections, and sepsis (Janda and Abbott, 2010; Figueras and Beaz, 2015; Fernández, 2020; Pessoa et al., 2022). It is capable of infecting both immunocompromised and immunocompetent individuals. While the global prevalence of

Aeromonas infections remains uncertain, research in California (1998) revealed an annual incidence rate of 10.5 cases per million individuals (King et al., 1999; Janda and Abbott, 2010). In England (2004), the incidence of *Aeromonas* bacteremia was reported at 1.5 cases per million individuals (Janda and Abbott, 2010), while in France (2006), it was lower at 0.66 cases per million (Lamy et al., 2009). Taiwan (2008) reported a notably higher incidence rate of *Aeromonas* bacteremia at 76 cases per million persons (Wu et al., 2014).

A variety of virulence factors, including the pili and flagella, Type III secretion system (T3SS), outer membrane proteins (OMPs), lipopolysaccharide (LPS), and extracellular components such as exo-toxin, aerolysins, haemolysins, enterotoxin, and siderophore, contribute to the intricate and multifaceted pathogenicity of *Aeromonas* infection (Chopra et al. 1999; Pablos et al. 2011; Peatman et al. 2018). The most important virulence factor in *A. hydrophila* is the crucial toxin aerolysin. Aerolysin and hemolysin are often linked to how harmful *A. hydrophila* is and plays a part in many infections in humans and aquatic animals (Rozi et al., 2018b; Sughra et al., 2022). Aerolysin (aerA) and hemolysin (Ahh1) genes have been identified in *A. hydrophila*, with studies showing a prevalence of 75% and 50%, respectively, in isolates from diseased fish (Sughra et al., 2022). Environmental conditions play a crucial role in modulating the expression of virulence genes, including aerolysin.

Aerolysin is a dimeric protein with a unique concentric double β -barrel structure. It is made up of 493 amino acids, which are highly conserved across the β -pore-forming toxin family. This structure is crucial for transitioning from a prepore to a mature pore, facilitating cell membrane penetration and subsequent cell lysis (Cirauqui et al., 2017). The biologically active mature toxin is responsible for the toxic effects of the bacteria that produce Act and aerolysin. The toxin then moves towards the cell and creates homo-heptameric pores on target cells, which can make them lose their osmotic balance, which leads to G-protein activation and cell death (Zhang et al., 2012). The absence of the gene that codes for aerolysin in certain strains significantly reduces their ability to infect other organisms, highlighting the importance of this toxin in the pathogenicity of certain bacteria (Howard et al., 2012). Several types of cells are vulnerable to aerolysin, such as epithelial cells, erythrocytes, fibroblast cells, lymphocytes, and granulocytes. This shows that aerolysin has a wide effect on host cells and that exposure could also be susceptible to its destructive effects (Howard et al., 2012). Understanding the correlation between environmental factors and the expression of

aerolysin genes is crucial for addressing *A. hydrophila* infections in aquaculture environments and formulating effective prevention and treatment plans.

The misuse of antibiotics exacerbates the issue of bacterial resistance, with *A. hydrophila* serving as a prime example. *A. hydrophila* has developed resistance to multiple antibiotics, including penicillins, cephalosporins, and carbapenems, penicillins, cephalosporins, lincosamides, nalidixic acid, and complicating treatment options ((Blake *et al.*, 2024; Sagas *et al.*, 2024). *A. hydrophila* has extended-spectrum cephalosporin resistance, which poses a significant challenge for healthcare providers in effectively treating infections caused by *A. hydrophila* (Chen *et al.*, 2024). On the other hand, vaccine production is essential to tackle the growing prevalence of *A. hydrophila* infections and the escalating antibiotic resistance rates in fish. Research and development of new antibiotics and alternative treatment options are essential to addressing bacterial resistance and effectively treating infections in the future. Traditional vaccine production takes years to synthesize and is much more expensive, leading to delayed and limited availability to aquaculture, resulting in increased infection and resistance rates (Laxminarayan *et al.*, 2024). Despite numerous experimental attempts, no commercial subunit vaccines are available for *A. hydrophila* in Indonesian aquaculture. The development of vaccines is hindered by the complexity of inducing protective immune responses (Nayak, 2020).

The development of vaccines against *A. hydrophila* is challenging due to its intracellular nature and ability to evade the immune system. Traditional vaccine approaches face difficulties in targeting this pathogen effectively, necessitating innovative strategies to overcome these hurdles. Recent research has explored various methods, including reverse vaccinology, multi-epitope vaccines, live-attenuated strains, and novel delivery systems. An effective and protective vaccine must meet the essential parameters (Gasperini *et al.*, 2021). Recent reverse vaccine technology uses genomic information to prioritize potential vaccine targets without culture (Qamar *et al.*, 2020). Traditional vaccine technology is costly, time-consuming, and requires a lot of human resources (Bidmos *et al.*, 2018). Using genome-based reverse vaccination techniques is quite beneficial in uncovering new vaccine targets that are difficult to find through traditional vaccine development (Saadi *et al.*, 2017). For safety and effectiveness reasons, researchers test potential vaccines before putting them through clinical trials (Chakraborty *et al.*, 2023) using molecular dynamics simulations and reverse vaccination. Researchers successfully developed a meningococcal

serogroup B (4CMenB) vaccine (Serruto *et al.*, 2012) and a COVID-19 vaccine (Chakraborty *et al.*, 2023) using the reverse vaccination approach. In recent years, reverse vaccination, or multi-epitope vaccines (MEVs), have proven useful in finding new vaccine targets and reducing vaccine failure rates in clinical trials (Reker *et al.*, 2014). However, no previous research is related to designing a multi-epitope vaccine targeting aerolysin against *A. hydrophila* by employing subtractive proteomics, reverse vaccinology, and immunoinformatics approaches. Given the importance of aerolysin and its destructive effects, designing an MEV against it could reduce the infection rate in the community by eliciting cell-mediated and humoral immunity. Innovative approaches, such as in silico design of multi-epitope vaccines targeting the aerolysin toxin, show promise in eliciting robust immune responses against *A. hydrophila*. While MEVs show promise in silico, transitioning from computational predictions to real-world applications requires extensive in vitro and in vivo validation to confirm efficacy and safety (Karkashan, 2024).

This study focuses on developing a multi-epitope vaccine (MEV) against *A. hydrophila* aerolysin toxin by improving cell-mediated immunity and humoral immunity (antibody). Aerolysin is identified as the most toxic virulence factor of *A. hydrophila*, contributing to various infections such as septicemia, gastroenteritis, and wound infections in humans, as well as diseases in aquatic animals (Abdella *et al.*, 2023; Alawam and Alwethaynani, 2024). Advanced computational methods such as immunoinformatics, subtractive proteomics, and reverse vaccinology have been used to develop multi-epitope vaccines targeting aerolysin against *A. hydrophila*. These approaches have shown promise in designing vaccines that elicit robust immune responses and potentially combat antibiotic-resistant strains of *A. hydrophila* (Zhang *et al.*, 2022). In addition, further research could focus on optimizing multi-epitope vaccine delivery systems to ensure maximum effectiveness and long-term protection. Collaboration between researchers in fields such as immunology, bioinformatics, and microbiology will be crucial in advancing the development of new vaccines against this pathogen. Our research has shown promising results, indicating that the vaccine effectively suppresses the onset and progression of *A. hydrophila* infection in healthy and already-infected individuals. The vaccine showed high binding affinity to immune system receptors, indicating strong immunogenicity. In addition, the in silico cloning process using SnapGene enabled efficient production of the vaccine candidate. Overall, our findings support the potential use of this vaccine to combat *A. hydrophila* infection, which offers hope for improving future pre-

vention and treatment strategies.

2. Materials and Methods

2.1 Materials

The tools used in this research were Eppendorf centrifuge 5430R, Haaken LD5 water bath, Onemed® microtube PCR 0.2 µL, Onemed® microtube polymerase chain reaction (PCR) 1.5 mL, comb, plate, UV transilluminator Flowgen, Microwife Sharp, Mupid EXU submarine (horizontal) type electrophoresis system advance, the Modern Thermal Cycler (Flex Cycler2) by Analytikjena. The materials used in this research were goramy fish, AHSA1, and ATCC 35654 isolate with a density of 10^8 CFU/ml, iNtRON Biotech® G-Spin™ for bacteria Genomic DNA Extraction Kit (G-buffer, binding buffer, washing buffer A, washing buffer B, elution buffer), Himedia® agarose gel, Merck® TBE Buffer 10x, Marker Analytikjena® innuSTAR1 kb DNA Ladder express analytikjena, Smobio® Flour vue™ nucleic acid gel stains 1001, Bremis® parafilm, the macrogen forward-reverse PCR genekit, Promega Nuclease Free Water, GoTaq® G2 Green Master Mix (Promega), and DNA extraction.

2.1.1 Ethical approval

This experiment was conducted under approval No. 170-Kep-UB-2024 by the Animal Care and Use Committee, Brawijaya University, Indonesia.

2.2 Methods

2.2.1 Bacterial isolation and sampling of goramy

The study involved 43 live specimens of naturally infected goramy collected from a local fishpond in Gunung Sari, Surabaya, Indonesia ($7^{\circ}18'8''$ LU; $112^{\circ}42'51''$ E). The fish showed hemorrhagic ulceration, swollen abdomen, exophthalmia in eyes, fluid accumulation in the abdomen, swollen liver and spleen, and water-filled intestines. The breakdown of goramy specimens was euthanized by administering an excessive amount of clove oil that had been previously utilized for bacterial isolation. Following sedation, the afflicted fish were thoroughly rinsed with 70% ethyl alcohol in a sterile manner, and the site of ulceration was treated with a hot scalpel to minimize contamination. Swabs were collected using a sterilized loop from the embolised body parts and kidneys after sterilization. These swabs were then streaked onto a culture medium by incubating them on Rimler-Shotts (RS) medium (Himedia, India). Incubation of the RS plates at $30 (\pm 2)^{\circ}\text{C}$ for 24-48 hours observed bacterial colony growth on the plates, characterized by solitary

yellow colonies. The selection and purification of two dominant growing bacterial colonies were achieved by subculturing them on the tryptic soy agar medium with repeated streaks. The selection and purification process resulted in the single colony being designated and labeled as isolate AHSA1. Additional biochemical and molecular identification procedures were performed on the AHSA1 and ATCC 35654 isolates. Furthermore, bacterial isolates were cultivated in LB broth (Himedia, India) supplemented with 10% glycerol and preserved at minus 80°C for extended periods.

2.2.2 Biochemistry of bacterial isolates

Pure cultures of AHSA1 and ATCC 35654 isolates were inoculated on NA medium overnight at 29°C , and colony morphology was observed. Isolates were subjected to Gram staining, followed by [Martin-Carnahan et al. 2015](#) by microscopic observation. Isolates from TSA plate media are continued with reisolation on selective media for gram-negative bacteria using MCA (MacConkey Agar). If the results are positive, reisolation will be carried out on *A. hydrophilla* selective media using RS Medium Base (Rimler-Shotts Medium Base). Single colony results are subjected to gram staining tests. Then biochemical tests using KIA media, Simon citra agar, urea, MR, VP, Sugars (glucose, sucrose, lactose, mannitol, maltose, sorbitol, inositol), catalase, oxidase, ornithine, lysine decarboxylase, arginine dehydrolase, and bile esculin, growth at 30°C , salt tolerance 6.5%, Novobiocin and O/129 susceptibilities test, H₂S production, starch hydrolysis, and urea ([Legario et al., 2023](#)) are conducted. The bacterial characters based on colony morphological observations, physiological properties, and biochemical properties testing were validated with *Aeromonas* sp. following ([Table 2](#)) ([Popoff and Véron 1976](#); [Abbott et al., 2003](#)).

2.2.3 Characterization of cell morphology

Scanning Electron Microscope (SEM) was performed to examine bacteria cell morphology using a Biorad Smart Spec Plus UV/VIS Spectrophotometer to determine optical density (OD) and concentration. OD values in the range of 0.18 with a concentration of 10^6 - 10^8 cells / mL can be used for testing. Stages of biological sample preparation include fixation, dehydration, drying, and coating with a conductive layer. Then, it was observed with a microscope Hitachi tabletop Microscope TM3000 magnification of 20,000x.

2.2.4 Molecular identification based on 16S rRNA and rpoB gene amplification

The genomic DNA from both AHSA1 and ATCC 35654 isolates, which were grown in LB medium at a temperature of 29°C overnight in an orbital shaker incubator, was extracted using the iNtRON Biotech® G-Spin™ according to the instructions provided by the manufacturer. The extracted DNA was then stored at a temperature of -20°C until it was ready to be used. The 16S rRNA gene was amplified using universal bacterial primers following established techniques. In contrast, the *rpoB* (RNA polymerase beta subunit) gene was amplified using the protocol described by Persson *et al.* (2015) (Table 1).

by adding a solution of 6.5 µl NFW and 12.5 µl GoTaq® G2 Green Master Mix (Promega) into a microtube and mixing until homogeneous. The aerolysin gene primer with forward primer and reverse primer (Table 1), two µl each, with a final concentration of 10 pmol and two µl DNA template. The PCR program for DNA amplification is as follows: initial denaturation at 94°C for 2 minutes, then denaturation at 94°C for 30 seconds, annealing at 57°C for 50 seconds, and extension at 72°C for 1 minute with 30 cycles, final extension 72 °C for 7 minutes final temperature 4°C. The

Table 1. List of identification primers by 16S rRNA, *rpoB*, and *aerA* genes

Target gene	Primer sequence (5' → 3')	References
16S rRNA	F AGAGTTTGATCCTGGCTCAG	Moreno <i>et al.</i> , 2002
	R ACGGCTACCTTGTTACGACTT	
<i>rpoB</i>	F GCAGTGAAAGARTTCTTTGGTC	Kupfer <i>et al.</i> , 1997
	R GTTGCATGTTNGNACCCAT	
<i>aerA</i>	F CCTATGGCCTGAGCGAGAAG	Wang <i>et al.</i> , 2003
	R CCAGTTCAGTCCCACCAC	

For each gene, the PCR reaction included 25 µl of pre-made using GoTaq® G2 Green Master Mix (Promega), 2.5 µl each of forward and reverse primers, five µl of DNA template, with the total volume adjusted to 50 µl using nuclease-free water. Additionally, a negative control was included where no DNA template was used. The PCR-amplified products for both genes were assessed for quality using 1% (w/v) agarose gel. The purified products were then sent to PT. Genetica Science, Indonesia, for Sanger sequencing. The gene data sets were modified using the Clustal W tool in MEGA 11 to align sequences for analysis. Furthermore, BLAST searches were conducted in the NCBI database to identify the closest relatives of the sequences for comparative analysis. Phylogenetic trees were constructed using the Neighbour-joining method with the Kimura 2-parameter (K2P) evolutionary sequence model to calculate evolutionary distances for accurate classification. The accuracy of the tree branches was confirmed through a bootstrap analysis involving 1000 replicates to assess the reliability of the phylogenetic relationships. The strains *Pseudomonas aeruginosa* KH3 (GenBank accession no. MN307278.1), *P. syringae* NCPPB 600 (GenBank accession no. FN433213.1), and *P. aeruginosa* ATCC 23993 (FJ652723.1) were selected as outgroups to establish the root of the tree based on the 16S rRNA and *rpoB* data.

2.2.5 Aerolysin gene PCR

Virulent gene amplification was carried out

PCR results were electrophoresed on a 1 % agarose gel and a voltage of 100 V for 30 minutes. The size of the base pair generated for Aer gene detection is 462 bp. The PCR stage stops at the extensive base pair reading that is visible, and then one of the *A. hydrophila* virulent gene application results is positive. Then, the process continues to the purification and sequencing stage. The sample PCR products were purified using the MicroClean DNA Purification Kit. A 100 µl PCR product was combined with 100 µl of microclean (1:1 ratio) and thoroughly mixed using a pipette until homogenous. An incubation period of 5 minutes at ambient temperature was followed by centrifugation at 13,000 rps per minute for 5 minutes. The supernatant solution was discarded, vortexed, and the remaining supernatant was discarded until entirely clear. The recovered pellet was resuspended in 30 µl of TE buffer to maintain DNA stability and stored at -20°C. The DNA of *A. hydrophila* aerolysin was purified and sequenced using an automated sequencer (Applied Biosystems Integr Model 310) following the Sanger sequencing method. The gene sequences obtained were edited using Clustal W (built-in in MEGA 11), and BLAST searches were performed in the NCBI database to identify their nearest neighbours. Phylogenetic trees were constructed based on the evolutionary distances of the gene sequences using the Neighbour-joining with the Kimura 2-parameter (K2P) evolutionary sequence model. Tree branches were authenticated by bootstrap analysis of 1000 replicates.

2.2.6 Retrieving aerolysin sequences

Aerolysin is a potential candidate for a MEV against *A. hydrophila*. Its pathogenicity was verified using the Virulence Factor Database, which contains thousands of bacteria linked to various diseases (Liu et al., 2022). The Aerolysin amino acid sequence of *A. hydrophila* was retrieved from NCBI fasta with APJ13760.1 accession numbers (<https://www.ncbi.nlm.nih.gov/protein/APJ13760.1>) (Cao et al., 2020). Homology tests were performed with three types of lactobacilli using the NCBI server's BLASTp application: *Lactobacillus casei*, *L. rhamnosus*, and *L. johnsonii*. The investigation aimed to verify the aerolysin sequence homology to natural flora, fish, and humans, as acquired epitopes could activate the immune system or cause autoimmune (Mahram, 2015). Conservation analysis was performed on aerolysin to determine its presence in other variations within the *Aeromonas* genus. The results could increase the importance of a MEV based on aerolysin, potentially providing complete protection against *Aeromonas* strains that contain aerolysin.

2.2.7 Immune epitope prediction

Prediction of B and T cell epitopes is an important process in vaccine design. Through the prediction of B and T cell epitopes, cellular and humoral immune responses to antigens will be obtained (Jespersen et al., 2017). B-cell epitopes play an important role in vaccine design and production. The IEDB web server (<http://tools.iedb.org/main/bcell/>) was used to predict B cell epitopes. This prediction is necessary because B lymphocytes are one of the main factors of the immune system (Dhanda et al., 2019). B cell epitopes were identified in the yellow zone if they exceeded a threshold value of 0.5. In contrast, sequences in the green region below this threshold were not considered B cell epitopes. The results of the B epitope were then used for T epitope prediction via the IEDB web server (<http://tools.iedb.org/main/tcell/>) to determine the binding ability of the B cell epitope to MHC-I and MHC-II. Peptides were selected based on low percentile values because the lower the percentile value, the stronger the bond (Vita et al., 2015). Peptides were screened with a number range <1 for MHC-I and <10 for MHC-II. The method predicts epitopes from a wide range of immune system alleles, enhancing the versatility of the MEV for experimental methods (Dey et al., 2022). Epitopes were chosen based on low percentile ranking, ensuring maximum binding to immune receptors, thereby enhancing the applicability of the MEV (Sidney et al., 2008; Wang et al., 2010).

2.2.8 Antigenicity, allergenicity, water solubility, and

toxicity analysis

Filtering epitopes for multi-epitope vaccines (MEV) involves several analytical steps to ensure their safety and efficacy. This includes assessing antigenicity, toxicity, solubility, and allergenicity. Computational tools like Vexigen 2.0, ToxinPred, and Allertop 2.0 play a crucial role in this process, as they help evaluate these properties efficiently. Vexigen 2.0 is used to evaluate the antigenicity of epitopes, ensuring they can elicit an immune response. Epitopes with an antigenicity value of less than or equal to 0.4 are considered for further analysis (Doytchinova et al., 2005). ToxinPred is employed to assess the toxicity of epitopes, filtering out those that may pose a safety risk (Rathore et al., 2024). The Innovagen Peptide Calculator determines the solubility of non-toxic epitopes with acceptable antigenicity. Soluble epitopes are crucial for effective vaccine formulation, as they ensure proper delivery and stability (Collatz et al., 2021). Allertop 2.0 is used to screen for potential allergic reactions. Only epitopes that test negative for allergenicity proceed to further processing, ensuring the vaccine's safety for individuals with allergies (Dimitrov et al., 2014).

2.2.9 Physicochemical properties analysis

The analysis of the physicochemical properties of vaccine constructs is crucial for understanding their stability, efficacy, and manufacturability. These properties include molecular weight, pK values, instability indices, GRAVY values, isoelectric pH, hydrophobic properties, approximate half-life, and aliphatic index. The ExPASy ProtParam tool is often used to calculate these properties, providing insights into the vaccine's behavior in biological systems. This analysis is essential for optimizing vaccine design and ensuring effective immune responses. Utilizing the ExPASy ProtParam web server, the vaccine constructs' physicochemical characteristics were examined to functionally characterize them (<http://expasy.org/cgi-bin/protparam>) (Gasteiger, 2005).

2.2.10 Final vaccine candidate

The process of finalizing a vaccine candidate sequence involves the strategic assembly of epitopes and the use of linkers and adjuvants to enhance immunogenicity and stability. This approach is crucial for developing vaccines that can elicit strong immune responses, both cellular and humoral. Using computational tools and simulations plays a significant role in predicting and validating the efficacy of these vaccine constructs. Multi-epitope vaccines are designed by selecting non-toxic, antigenic, non-allergenic, and

immunogenic epitopes. These epitopes are linked using specific linkers like GPGPG to maintain stability and prevent self-complementary binding (Zhu *et al.*, 2024; Dashti *et al.*, 2024). The selection of epitopes is guided by immunoinformatics tools, which help predict B-cell and T-cell reactivity, ensuring broad immunogenicity and safety (Nguyen and Kim, 2024; Mortazavi *et al.*, 2024). Linkers such as EAAAK and GPGPG connect epitopes and adjuvants, enhancing the vaccine's stability and immunogenicity. The EAAAK linker was used to conjugate adjuvants to the first epitope and Cholera toxin B were used as an adjuvant to further boost immune responses (Stratmann, 2015; Mortazavi *et al.*, 2024). Adjuvants are crucial for enhancing the vaccine's ability to elicit a robust immune response, as demonstrated in various studies where they are integrated into the vaccine construct (Zhang *et al.*, 2022; Zhu *et al.*, 2024). Computational tools like c-IMMSIMM stimulate immune responses, providing insights into the vaccine's potential to induce both humoral and cellular immunity. These simulations help predict the vaccine's efficacy before experimental validation (Zhu *et al.*, 2024; Zhang *et al.*, 2022).

2.2.11 *In silico* immune response

The MEV construct was analysed using the C-ImmSim server to determine if its epitopes could produce immunity. The construct elicited potent cellular and humoral immune responses, with an increase in adaptive responses like IgM antibodies. Additionally, robust cellular immune responses were observed, with significant interferon-gamma, IL-10, and IL-2 production within five days post-administration. These findings suggest MEV's potential as an effective vaccine candidate.

2.2.12 Structure of 3D and structure refinement

To create a 3D protein structure model, you can use the I-TASSER web server (<https://zhang-group.org/I-TASSER/>) and Swiss Model servers (<https://swissmodel.expasy.org/>). I-TASSER creates a structural model through 4 steps, namely threading, structural assembly, model selection, and refinement (Zheng *et al.*, 2019). SWISS-MODEL predicts the chemical quality of the multi-epitope vaccine model using the Ramachandran plot, which illustrates the theoretical conformation of an amino acid residue (Waterhouse *et al.*, 2018). Tertiary structure refinement of the vaccine design was performed using the GalaxyRefine web server (<https://galaxy.seoklab.org/>)

2.2.13 Molecular docking

Molecular docking was utilized to assess the binding affinity of the Multi-epitope Based Vaccine (MEBV) with the immune cell receptor (TLR), ensuring the construct's effectiveness (Nguyen and Kim, 2024). Molecular docking and docking refinement can be done with the help of the ClusPro server and a visualization cartoon view of the docking between immune responses and MEV multi-epitope vaccine (MEV) using the PyMol software. Interphase between antigenic molecules is based on molecular docking and can produce an effective immune response (Jalal *et al.* 2022). Molecular docking of the vaccine was performed with TLR4 (PDB: 4G8A), TLR9 (PDB: 8AR3), MHC-I (PDB: 1L1Y), and MHC-II (PDB: 1KG0) receptors (Kozakov *et al.*, 2019).

2.2.14 *In silico* cloning and codon optimization

The JCAT (Java Codon Adaptation Tool) was used to back-translate the vaccine sequences into cDNA to improve the expression of constructed vaccine proteins in the *E. coli* system (Grote, 2005). The JCAT tool was used to determine the GC contents of DNA sequence and Codon Adaption Index score (CAI) for the optimized nucleotide sequence while avoiding the prokaryotic ribosome binding sites and Rho-independent termination of transcription cleavage site for restriction enzymes (Fei *et al.*, 2020). The pET-28a(+) vector was used to ensure the vaccine construct cloning and expression in *E. coli* using the Snapgene tool.

3. Results and Discussion

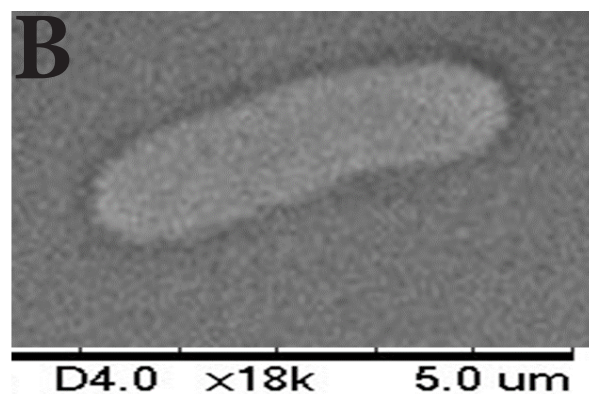
3.1 Results

3.1.1 Morphological and biochemical characterization

The prevailing colonies were derived from two bacterial isolates, AHSA1 and ATCC 35654, which exhibited a circular shape with an average diameter of 2-3 mm and appeared yellowish on nutrient agar. Based on comparisons and their characteristics, the two isolates were identified as *A. hydrophila*, following Austin and Austin (2016). These characteristics include a beige colony colour, convex elevation, smooth inner structure, production of gas and H₂S, fermentation, positive results in catalase and oxidase, oxidative, motility, indole, Novobiocin susceptibility, Arginine, Voges Proskauer (VP), Aesculin, growth at 30°C, salt tolerance 6.5% NaCl, and Simmons Citrate test. However, it yielded negative results in the urea, Lysine and Ornithine decarboxylation, O/129 disk susceptibility, and methyl red (MR) test. The glucose, sucrose, lactose, and maltose tests yielded positive results, whereas the mannitol, inositol, and sorbitol tests yielded negative results (Table 2).

Table 2. Biochemical characteristics of bacteria isolates (AHSA1) isolated from goramy

Characters	Popoff and Veron, 1976	Isolate AHSA1
Gram stain	-	-
Shape	Rod	Rod
Motility	+	+
Oxidase	+	+
Catalase	+	+
Urea	-	-
Citrate utilization	+	+
Oxidative - Fermentative Test	ND	Oxidative
Arginine decomposition	+	+
Lysine decarboxylation	-	-
Ornithine decarboxylation	-	-
Esculin hydrolysis	+	+
Starch hydrolysis	ND	+
Methyl-red test	-	-
Voges-proskaur	+	+
Indole	+	+
H ₂ S production	+	+
Growth at 30°C	+	+
Salt tolerance (6.5% NaCl)	ND	-
Novobiocin susceptibility test	+	+
O/129 Disk Susceptibility Test	-	-
Acid and gas production from glucose	+	+
Acid production		
Lactose	+	+
Sucrose	+	+
Maltose	+	+
Mannitol	-	-
Inositol	-	+
Sorbitol	-	+
Similarity Percentage		92.85%

**Figure 1.** Isolation *A. hydrophila* from goramy (A), Morphology of *A. hydrophila* cells observed by SEM, magnification 20,000x with scale Bar 5 μ m

The confirmation test was extended using a SEM at a magnification of 20,000x to observe the cellular structure of *A. hydrophila*. The observation revealed rod-shaped bacteria with dimensions ranging from 0.4 to 1.0 microns in width and 2.39 microns in length (Figure 1).

3.1.2 Molecular identification utilising 16s rRNA and rpoB genes

The genomic DNA from both isolates was subjected to PCR amplification using universal bacterial 16S rRNA primers, producing amplicons measuring around 1505 base pairs. The BLAST analy

sis of 16S rRNA and rpoB sequences indicated that isolate AHSA1 was identified as *A. hydrophila* with the highest similarity to other *A. hydrophila* strains in the Genbank database. The *A. hydrophila* AHSA1 strain from Surabaya, East Java, Indonesia, had 16S rRNA and rpoB gene sequencing data that revealed 99.23–99.68% similarity with eleven reference strains and 99.41% similarity with ATCC 35654: *A. hydrophila* strain MFB, Argentina (GenBank accession no. KU942608.1), *A. hydrophila* strain SG11, Brazil (GenBank accession no. HE681732.1), *A. hydrophila* strain M_45, China (GenBank accession no. MG428936.1), *A. hydrophila* strain z83c, Japan (GenBank accession

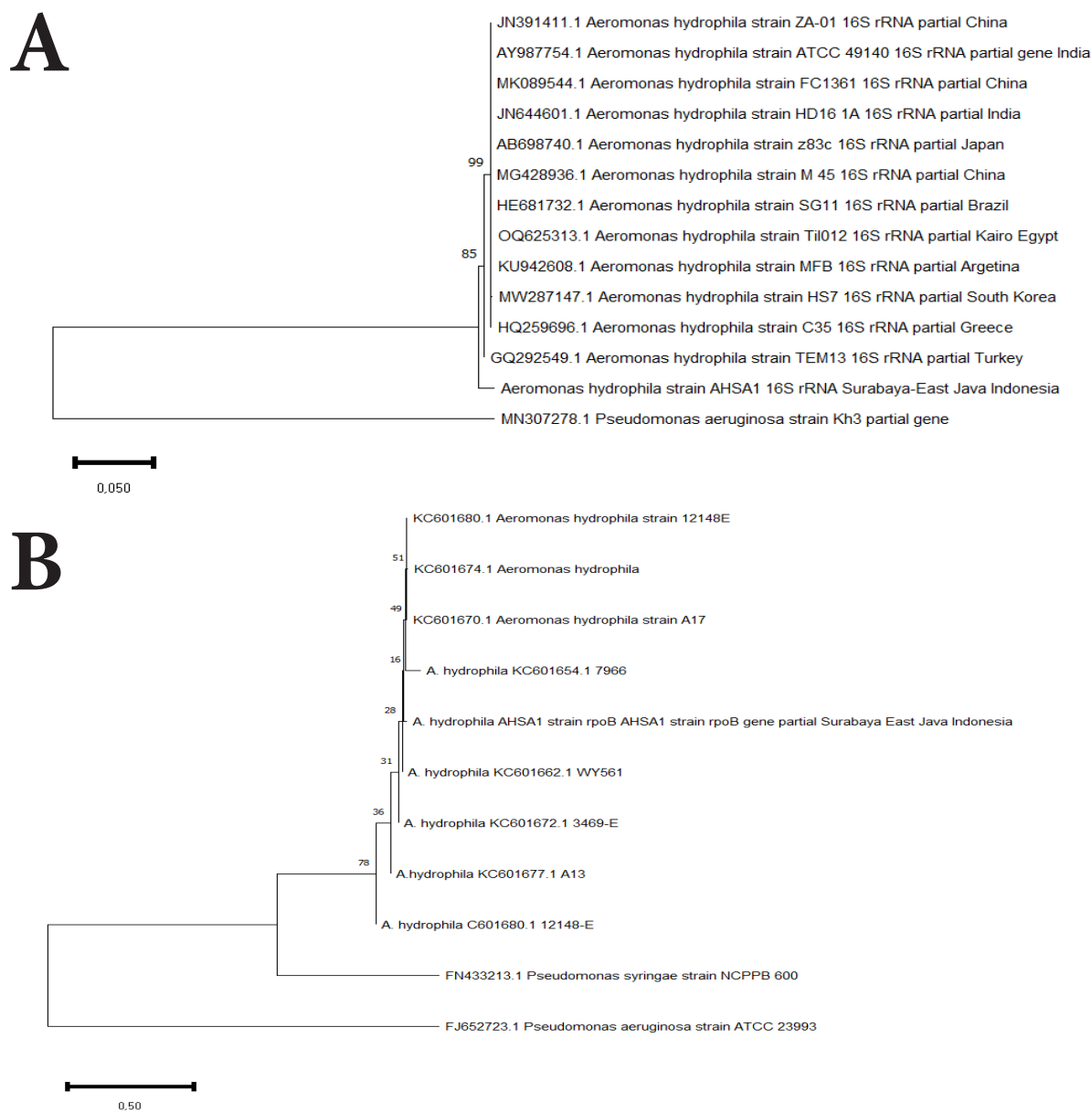


Figure 2. Phylogenetic tree (UPGMA model) based on 16S rDNA (a) and rpoB (b) of a bacterial isolate (AHSA1) of *A. hydrophila* and closely related comparator species *P. aeruginosa* and *P. syringae* were selected as outgroups for the 16S rDNA (a) and rpoB genes. Percentage bootstrap values (1000 replicates) are shown at each branch point.

no. AB698740.1), *A. hydrophila* strain HD16_1A, India (GenBank accession no. JN644601.1), JN644601.1), *A. hydrophila* strain FC1361, China (GenBank accession no. MK089544.1), *A. hydrophila* strain ZA-01, China (GenBank accession no. JN391411.1), *A. hydrophila* strain C35, Greece (GenBank accession no. HQ259696.1), *A. hydrophila* strain HS7, South Korea (GenBank accession no. MW287147.1), *A. hydrophila* strain Til012, Cairo Egypt (GenBank accession no. OQ625313.1), *A. hydrophila* strain TEM13, Turkey (GenBank accession no. GQ292549.1), and *A. hydrophila* strain ATCC 49140 (GenBank accession no. AY987754.1). Furthermore, the polymerase chain reaction (PCR) amplification of the *rpoB* gene resulted in the production of approximately 558 base pair (bp) amplicons from both isolates. The AHSA1 againsts ATCC 35654 gene showed 100% coverage with 99.50% and 99.41% similarity to *A. hydrophila* strain 3469-E (GenBank accession no. KC601672.1), *A. hydrophila* strain WY561 (GenBank accession no. KC601662.1), *A. hydrophila* strain 7966 (GenBank accession no. KC601654.1), *A. hydrophila* strain 12148E (GenBank accession no. KC601680.1), *A. hydrophila* strain A17 (GenBank accession no. KC601670.1), and *A. hydrophila* (GenBank accession no. KC601670.1). *A. hydrophila* (GenBank accession no. KC601674.1), *P. syringae* strain NCPPB 600 (GenBank accession no. FJ652723.1), and *P. syringae* strain NCPPB 600 (GenBank accession no. FJ652723.1), and *P. aeruginosa* strain ATCC 23993 (GenBank accession no. FJ652723.1). We recovered nearly the 16S rRNA and *rpoB* gene sequences for both isolates, with less than 1% of locations being undefined. The phylogenetic tree (Figure 2a, 2b) classified isolate AHSA1 as belonging to the same group as *A. hydrophila*. Significant bootstrap values further reinforced the clustering.

3.1.3 Molecular identification of the aerolysin gene using PCR

The PCR results obtained from selected AHSA1 and ATCC 35654 isolates were analysed using electrophoresis on a 1% agarose gel, along with a 100 bp ladder, to determine the size of the DNA fragments. A band with an amplicon size of 462 bp was found upon gel electrophoresis, as depicted in Figure 3. This observation confirms the presence of the pathogenic aerolysin gene of *A. hydrophila* in the two isolates. The gel electrophoresis results are illustrated in Figure 3, showing the bands corresponding to the test samples in lane 2 and lane 3 (AHSA1 and ATCC 35654 isolates).

3.1.4 Analysis and retrieval of aerolysin to construct a vaccine

The sequence of aerolysin obtained from the NCBI is available in the Protein Data Bank (PDB),

facilitating detailed structural analysis, as shown in Table 3. The alignment of aerolysin with various strains of the *Aeromonas* family revealed its presence in multiple pathogenic strains known to cause serious infections in humans and fish as hosts. The sequence did not show similarity with human and fish proteome or important normal flora bacteria like *Lactobacillus* species, indicating its safety for further analysis and vaccine development. Aerolysin was found in 17 *A. hydrophila* strains, 39 *Aeromonas* spp. Strains and other pathogenic *Aeromonas* strains, with alignment of sequences varied from 94% to 98%, confirm this virulence factor's presence in these strains. The conservation of aerolysin across strains ensures that a vaccine targeting this factor could protect against a wide range of infections caused by *Aeromonas*, addressing the challenge of strain variability (Zhang et al., 2022).

3.1.5 The B and T cell epitope prediction

The chosen proteins were prioritized for the immunological epitope prediction by initially predicting B cell epitopes and then T cell epitopes. Additional processing was conducted on B cell epitopes to discover T cell epitopes. Helper T lymphocytes boost B cells, macrophages, and cytotoxic T lymphocytes. In contrast, cytotoxic T cells can directly identify antigens. B cells can undergo differentiation and transform into plasma cells responsible for antibodies' production. Aerolysin is subjected to B cell epitope prediction. The sequence underwent filtration and was divided into 14 anticipated linear B cell epitopes, as demonstrated in Table 4. Figure 5 provides a schematic representation of all epitopes. The MHC-II and MHC-I epitopes acquired are displayed in Table 5.

- B-cell epitope prediction

The prediction of B-cell epitopes was conducted utilizing the Immune Epitope Database and Analysis Resource (IEDB) online platform, accessible at www.iedb.org. Twelve potential peptides (Pep1 to Pep12) were identified in this study by examining B-cell epitope prediction using the amino acid sequence of *A. hydrophila* aerolysin protein. The B cell epitope prediction output data differed between the two BepiPreds algorithms. A schematic representation of all the epitopes was also provided in Figure 4, indicating that sequences in the yellow region above the 0.5 threshold value are regarded as B-cell epitopes. In contrast, sequences in the green region below the threshold do not fall into the B-cell epitope category (26). A total of 252 amino acids (chosen from chains A and B of aerolysin) out of the 493 amino acids of aerolysin were further processed independently for MHC-II and MHC-I epitope prediction. T-cell epitope prediction was performed using all 252 B cell epitopes.

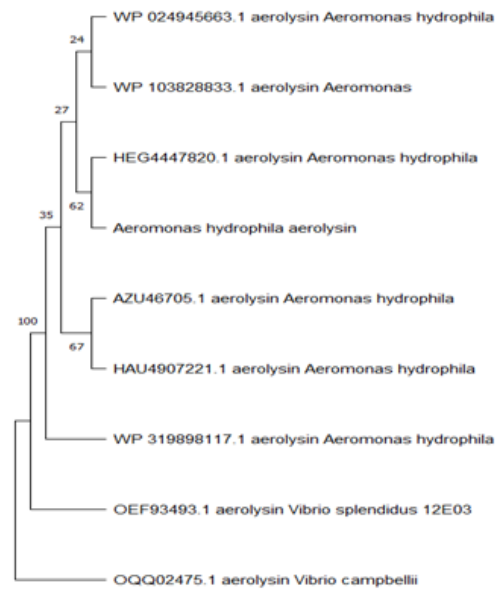
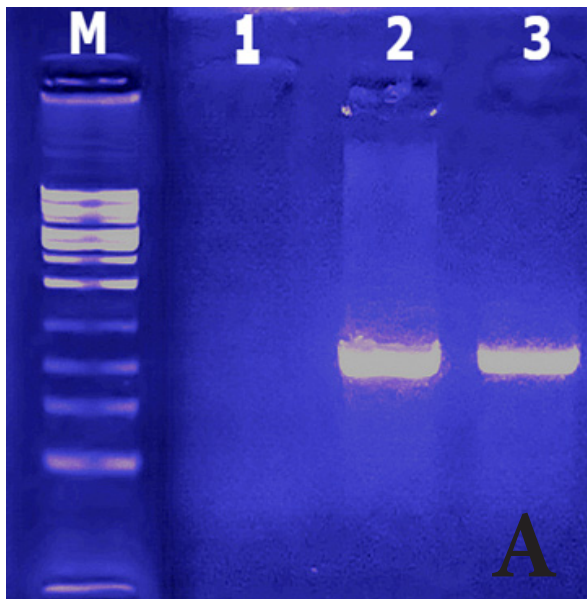


Figure 3. Detection of Aerolysin (*aerA*) gene in on 1.0 % agarose gel. A) Lanes M: Ladder (100 bp), 1: Control negative, 2: Control positive: *A. hydrophila* ATCC 35654 strain, 3: Amplifikasi PCR Aerolysin gene of *A. hydrophila* AHSA1 strain (462 bp) (A). Phylogenetic tree (UPGMA model) based on aerolysin gene (B)

Table 3. The amino acid sequence of aerolysin.

Virulence factor	Sequence of <i>A. hydrophila</i> Aerolysin Amino acid
>APJ13760.1 aerolysin <i>A. hydrophila</i> (<i>aerA</i>)	MQKLKITGLSLIISGLLMAQAHAAEPVYPDQLRFLSLGQEVCGDKYRPVTREEAQS VKSNIINMMGQWQISGLANGWVIMGPGYNGEIKPGSASNTWCYPVNPVTGEIPTLSALDIPDGDEVDVQWRLVHDSANFIKPTSYL AHYLG YAWVGGNHSQYVGEDMDVTRDGDGWVIRGNNDGGCEGYRCGEKTAIKVSNFAYNLDPDSFKHGDVTQSDRQLVKT VVGWAINSDTPQSGYDVTLRYDTATNWSKNTYGLSEKVT TKNKFKWPLVGETEL SIEIAANQSWASQNGGSTTT SLSQSVRPTV PARSKIPVKIELYKADISYPYEFKADVSYDLTSLGFLRWGGNAWYTHPDNRPNWNHTFVIGPYKDKASSIRYQWDKRYIPGEVKWWDWNWTIQQNGLSTMQNNLARVLRPV RAGITGDFSAESQFAGNIEIGAPVPLAADSKVRRRTRSVDGAGQGLRLEIPLDAQELSGLGFSNVLSVTPAANQ

Tabel 4. Peptides sequence-based B-cell epitope prediction using Bepipred Linear Epitope Prediction 2.0

No.	Start	End	Peptide	Length
1	23	56	AAEPVYPDQLRFLSLGQEVCGDKYRPVTREEAQS	34
2	85	94	NGEIKPGSAS	10
3	100	131	PVNPVTGEIPTLSALDIPDGDEVDVQWRLVHD	32
4	154	190	NHSQYVGEDMDVTRDGDGWVIRGNNDGGCEGYRCGEK	37
5	204	217	PDSFKHGDVTQSDR	14
6	230	237	DSDTPQSG	8
7	266	276	NKFKWPLVGET	11
8	285	298	NQSWASQNGGSTTT	14
9	348	361	GGNAWYTHPDNRPN	14
10	369	394	GPYKDKASSIRYQWDKRYIPGEVKWW	26
11	428	467	SAESQFAGNIEIGAPVPLAADSKVRRRTRSVDGAGQGLRLE	40
12	469	480	PLDAQELSGLGF	12

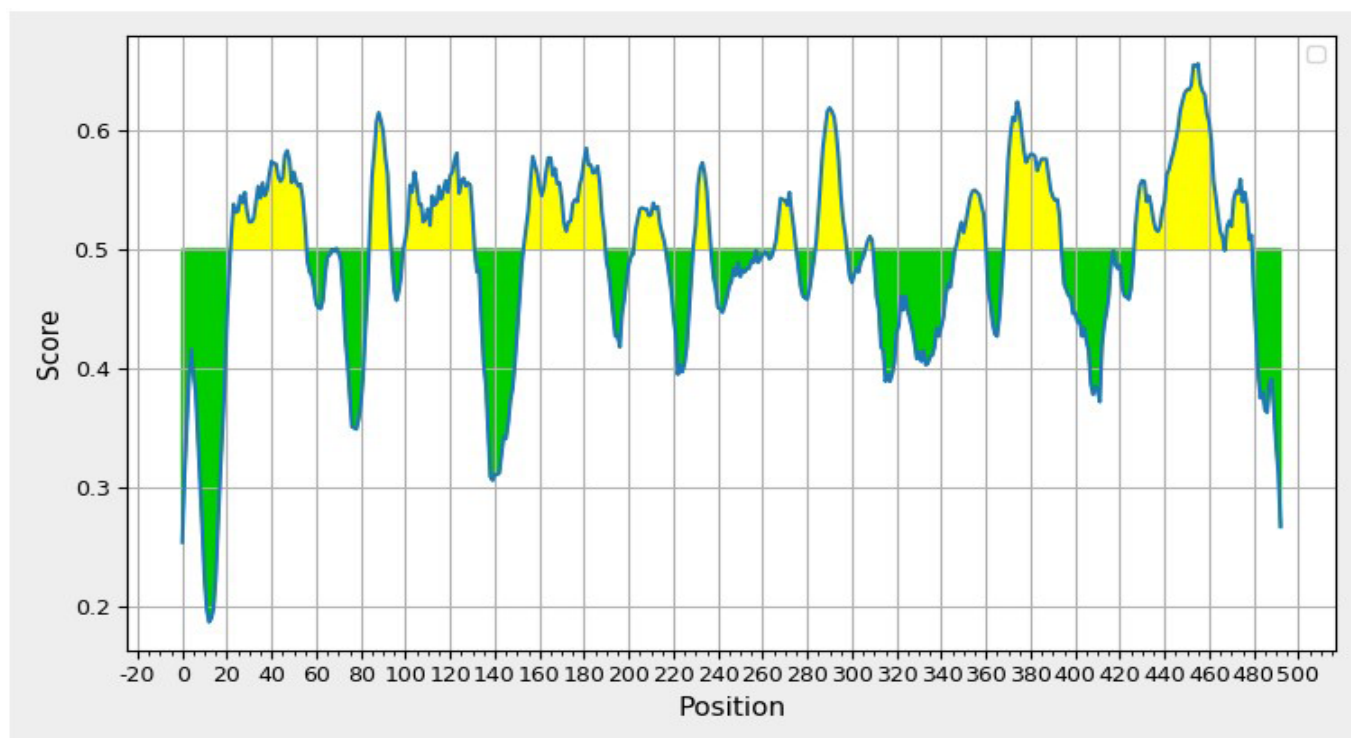


Figure 4. The individual score of discontinuous B cell epitopes was predicted in the multi-epitope subunit vaccine.

Table 5. Results of T cell epitope prediction analysis from Aerolysin amino acid sequence

MHC I				
Selected Epitopes	Antigenicity	Solubility	Toxicity	Allergenicity
DKASSIRYQW				
EIKPGSASPV				
EPVYPDQLRL				
KASSIRYQWD	ANTIGENIC	SOLUBLE	NON-TOXIN	NON ALLERGEN
NAWYTHPDNR				
KYRPVTREEA				
RLVHDNHSQY				
SVDGAGQGLR				
MHC II				
DGAGQGLRLEPLDAQ				
ADSKVRRTRSVDGAG				
DSKVRRTRSVDGAGQ				
AADSKVRRTRSVDGA	ANTIGENIC	SOLUBLE	NON-TOXIN	NON ALLERGEN
QYVGEDMDVTRDGDG				
GQGLRLEPLDAQELS				
HGDVTQSDRDSQTPQ				

- T Cell epitope prediction

The predicted epitopes were further analysed using the Immune Epitope Data Base (IEDB) computer tool to determine the potential interaction between the epitopes and T cells for MHC I and MHC II. In total, there were eight distinct T cell epitope sequences identified for the aerolysin (aerA) protein that can bind to MHC-I and seven epitope sequences for the aerolysin protein that can bind to MHC-II (Table 5). Subsequently, these prevalent epitopes were chosen for protein-peptide docking with MHC-I and MHC-II.

The T cell epitope sequence RLVHDNHSQY demonstrates the strongest binding affinity with MHC-I, with an antigenicity score of 0.91, suggesting its potential as a key component in vaccine design. Conversely, the epitope sequence EPVYPDQLRL exhibits the lowest score of 0.20. Based on the antigenicity scores provided, the peptides from highest to lowest antigenicity are Pep1 RLVHDNHSQY (0.91), Pep2 DKAS-SIRYQW (0.83), Pep3 NAWYTHPDNR (0.54), Pep4 KASSIRYQWD (0.40), Pep5 SVDGAGQGLR (0.37), Pep6 EIKPGSASPV (0.34), Pep7 KYRPVTRREEA (0.33), and Pep8 EPVYPDQLRL (0.20). These scores indicate the potential of these peptides to induce an immune response, with Pep1 and Pep2 having the highest antigenicity among the listed peptides.

The T-cell epitope DGAGQGLRLEPLDAQ had the highest antigenicity score of 4.00 for allele binding to MHC-II, while the epitope HGDVTQS-DRSDTPQ had the lowest value of 0.07. Additional peptide sequences at each epitope that exhibited antigenicity were deemed significant but not preferable as options for vaccine creation. The epitopes were predicted using MHC binding affinity, C-terminal truncation by the proteasome, and transport affinity. Predictions were made using MHC-I and MHC-II supertypes. The acceptable peptides are ordered based on their predictive value, which must be greater than 0.75.

3.1.6 The epitope screening

The host immune system can only be stimulated by antigenic proteins (Doytchinova *et al.*, 2007). To achieve this goal, we excluded all possible non-antigenic protein sequences from the study. We performed allergenicity and toxicity analyses to eliminate all toxic and allergic proteins and poorly water-soluble epitopes, thereby avoiding allergic and toxic responses (Dimitrov *et al.*, 2014; Ismail *et al.*, 2020). From a wide range of options, only the most favourable epitopes were chosen for our vaccine development. A total of 159 peptides were identified for MHC2 and 77 peptides for MHC1. Subsequently, the peptides underwent antigenicity, allergenicity, water solubility, and

toxin tests using a web server. Only those who passed the selection test were retained out of the 7 from 42 MHC2 and 8 MHC1 peptides. After a comprehensive assessment considering toxicity, solubility, allergenicity, and antigenicity, only a select few epitopes met the criteria for success. Table 5 displays the epitopes prepared to serve as the foundational material for our MEV.

3.1.7 The stage of vaccine construction

This work aimed to clarify the conserved epitopes that generate B and T cell responses, namely CD8+ and CD4+ responses. Furthermore, the epitopes that have been identified must not exhibit any undesired responses, such as autoimmune reactions, allergies, or toxicity. Hence, the primary factors for choosing the ultimate epitopes for vaccine creation are determined by the following parameters. (1) Full preservation of peptides in *A. hydrophila*, (2) utmost score for antigenicity, (3) positive score for immunogenicity, (4) high score according to the predicted algorithm, (5) epitopes with strong affinity for the most significant number of HLA alleles in the global population, (6) non-allergenic, and (7) non-toxic. B-cell epitopes and cytotoxic T lymphocytes (CTLs) were employed to create multi-epitope vaccination designs. One significant obstacle in the production of vaccines is that numerous modern subunit vaccines have a reduced ability to stimulate the immune system and produce immunological responses that are insufficient for providing protection. As a result, adjuvants are necessary to enhance the immune response.

Following the previously indicated analysis, we selected 15 of 51 distinct epitopes from the combined list. We overcame a significant obstacle by developing a vaccine construct that combined multiple epitopes with specific GPGPG linkers. We also used EAAAK linkers to connect epitope peptides and adjuvants to the cholera toxin B component. We positioned GPGPG linkers between the epitopes because they inhibit junction folding and trigger an immune response, including helper T cells. EAAAK is a peptide linker that forms a stable and inflexible α -helix structure. Intramolecular hydrogen bonds and a closed backbone distinguish it. Infusion proteins and EAAAK linkers serve as domain spacers. In addition, the linker enables the merging of epitopes to create a substantial structure with a polytope morphology. We used the cholera toxin B as an adjuvant because of its significant ability to boost IgA synthesis in the mucosa and other immune responses. It is non-toxic and can bind to the monosialotetrahexosylganglioside (GM1) receptor. This receptor is located in the cytoplasm and on the membranes of multiple cell types, including B cells, macrophages, dendritic cells, intestinal epithelial cells, and antigen-presenting cells. Similarly, the used

adjuvant poses no risks and triggers a strong immune response that targets the conjugated antigen. Figures 6A and 6B visually represent the MEV architecture, illustrating its structural components.

3.1.8 The physicochemical characteristics of the MEV

The physicochemical and solubility characteristics of the designed MEV were assessed utilizing the ProtParam web server. The molecular weight of the designed protein construct was calculated to be 54.50 kDa, indicating significant antigenic potential. With a theoretical isoelectric point (pI) of 5.75, the MEV is characterized as an essential protein with a net negative

immunogenic reactions in the body. An instability index exceeding 40 would indicate protein instability. The aliphatic index, calculated at 80.38, suggests a charge above pI and vice versa. The calculated instability index of 27.38 classifies the protein as stable, suggesting favorable characteristics for initiating highly thermostable protein (Ikai, 1980). The estimated half-life of the designed MEV construct is predicted to be 1 hour in mammalian reticulocytes in vitro and over 10 hours in *E. coli* in vivo. Additionally, the GRAVY value of -0.447 indicates the hydrophilicity of the protein (6). This negative GRAVY value confirms the hydrophilic nature of our construct (Kyte et al., 1982).

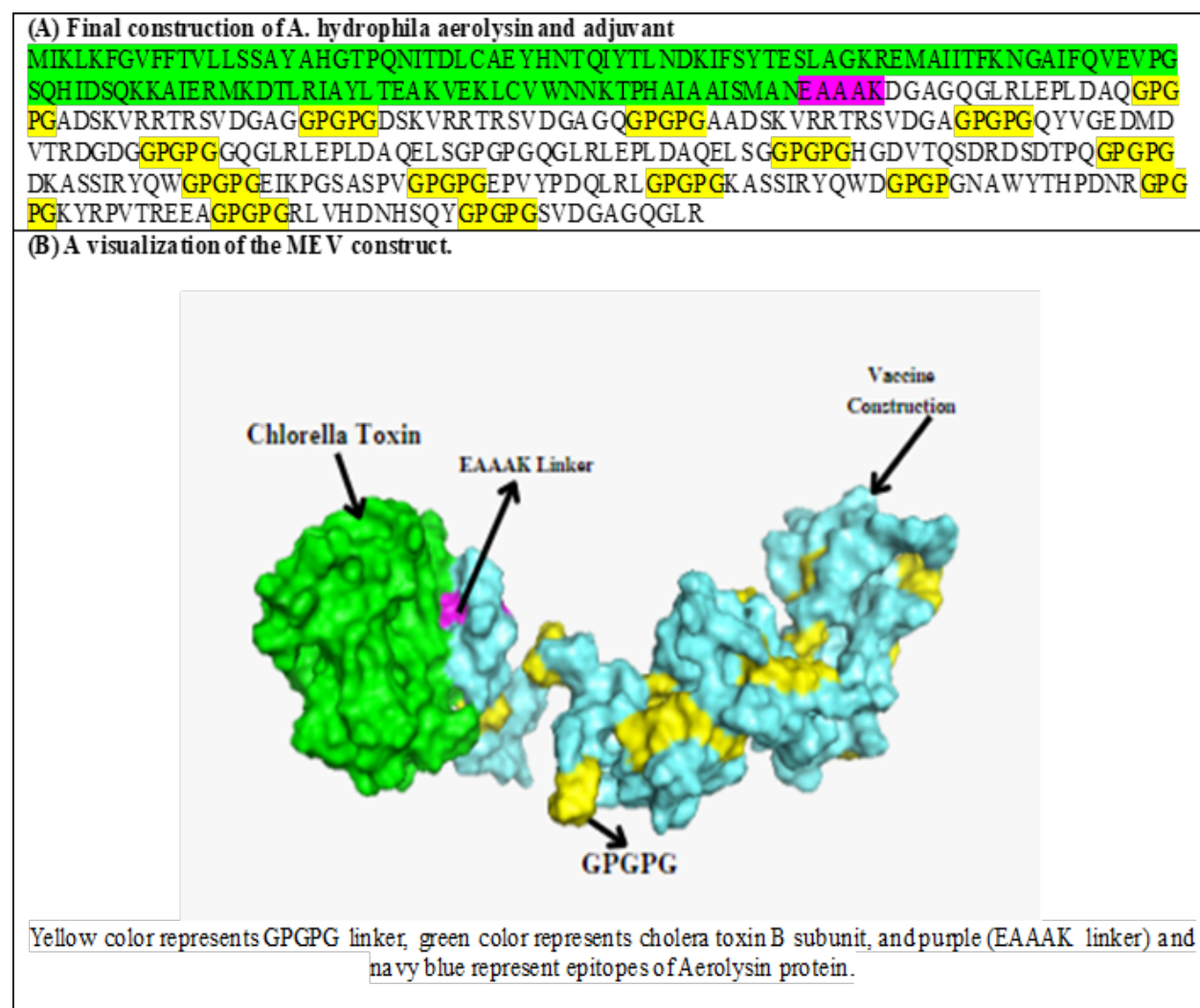


Figure 6. A visualization of the aerolysin MEV construct.

Table 6. Properties of the proteins used for the prediction of the immunodominant epitopes.

Accession No	Protein	No. of amino acids	MW	Instability Index	Antigenicity	Theoretical PI	GRAVY Score	Half-life
APJ13760.1	Aerolysin	493	54,509	10.49	Antigenic	5.75	-0.447	>10 h (<i>E. coli</i> , in vivo)

3.1.9 Modeling, refinement, and stability analysis of the vaccine structure

We used the MEV architecture to predict the structure by inputting the amino acids into the iTESSOR computer and employing ab initio modeling techniques. After refining the model structure, stability was evaluated using the Ramachandran plot and ERRAT score, indicating favorable values. The Ramachandran plot depicts the arrangement and distribution of amino acids in the MEV construct over distinct regions, each representing different degrees of stability. Four zones divide the plot: the most favored regions (red), additional allowed areas (brown), liberally allowed areas (yellow), and banned areas (pale). We determined the system's stability by including MEV construct residues in these regions. The diagram represents each residue's phi and psi angles, defining the residues' arrangement in different regions. The majority of the residues in the MEV build and Ramachandran plots showed that 85.25% of the residues were located in the most favorable regions, which was followed by the generously allowed zone (1.30%), the additional allowed regions (10.80%), and the forbidden regions (2.65%) (Figure 7). Figure 7 demonstrates the stability of our MEV construct by showing a higher number of residues in the permissible regions and a lower number in the forbidden regions.

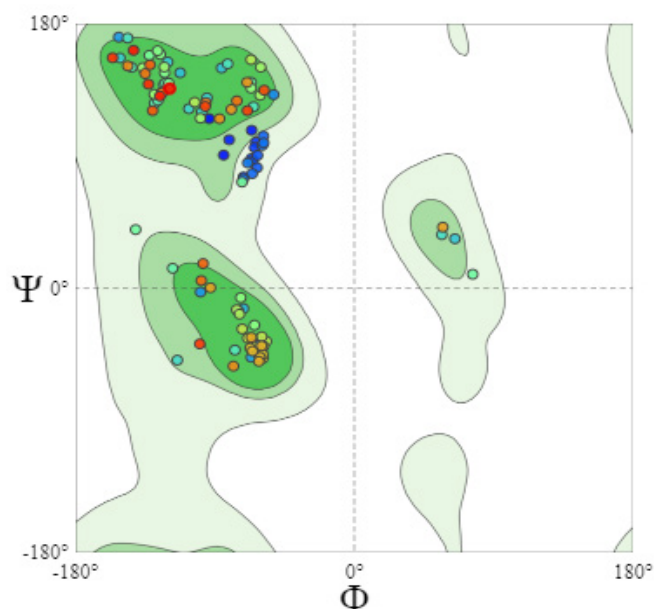


Figure 7. Ramachandran Plot of Aerolysin MEV Structure for stability analysis.

3.1.10 Immune simulation phase

We analysed the immunological response to the MEV using the C-ImmSim server to confirm that the epitopes would be sufficient to induce immunity

(Ashgar *et al.*, 2023). We can also use this approach to detect the emergence of immunological interactions between epitopes and specific targets. Figure 8B demonstrates the capacity of the MEV construct to elicit a robust cellular and humoral immune response. The simulation study that was done 35 days after the human immune system was virtually exposed to the highest dose of the vaccination antigen showed that adaptive responses, specifically IgG and IgM antibodies, grew faster. Also, within five days of the injection, there was a strong cellular immune response marked by significant production of interferon-gamma, interleukin (IL)-10, TNF-alfa, TGF-beta, and IL-2. The findings emphasize the MEV's capacity to provoke a robust immunological response, suggesting its potential as a promising vaccine candidate. This simulation provides a detailed representation of immune kinetics, including the role of specific antibodies and cytokines in the immune response, which can be essential for designing effective vaccines or treatments for fish and human diseases.

3.1.11 Molecular docking phase

The findings from molecular docking studies revealed that the MEV aerolysin protein construct exhibited a stronger affinity for TLR-4 than TLR-9, with a binding energy of -1081.4 and -723.2 kcal/mol. This binding energy of TLR-4 was significantly higher, suggesting a preferential interaction between the MEV protein. Additionally, the MEV protein displayed notable interactions with MHC-I and MHC-II, with binding energies of -866.2 kcal/mol and -9043.3 kcal/mol, respectively (Figure 9). The molecular docking data revealed that the MEV protein forms stable complexes with TLR-4, TLR-9, MHC-I, and MHC-II, characterized by multiple hydrogen bonds and hydrophobic interactions. These interactions contribute to the favorable binding energy observed and suggest a specific recognition mode between the MEV protein and its target receptors. The strong binding affinity of the MEV protein for TLR-4, TLR-9, coupled with its interactions with MHC-I and MHC-II, suggests its potential to activate diverse immune responses. These results collectively indicate that the MEV protein has the potential to engage with multiple immune receptors, suggesting its broad immunomodulatory capacity. These findings warrant further investigation to elucidate the precise mechanisms underlying the MEV protein's immunomodulatory effects and explore its therapeutic potential.

3.1.12 MEV expression and evaluation

The predicted MEV vaccine was subjected

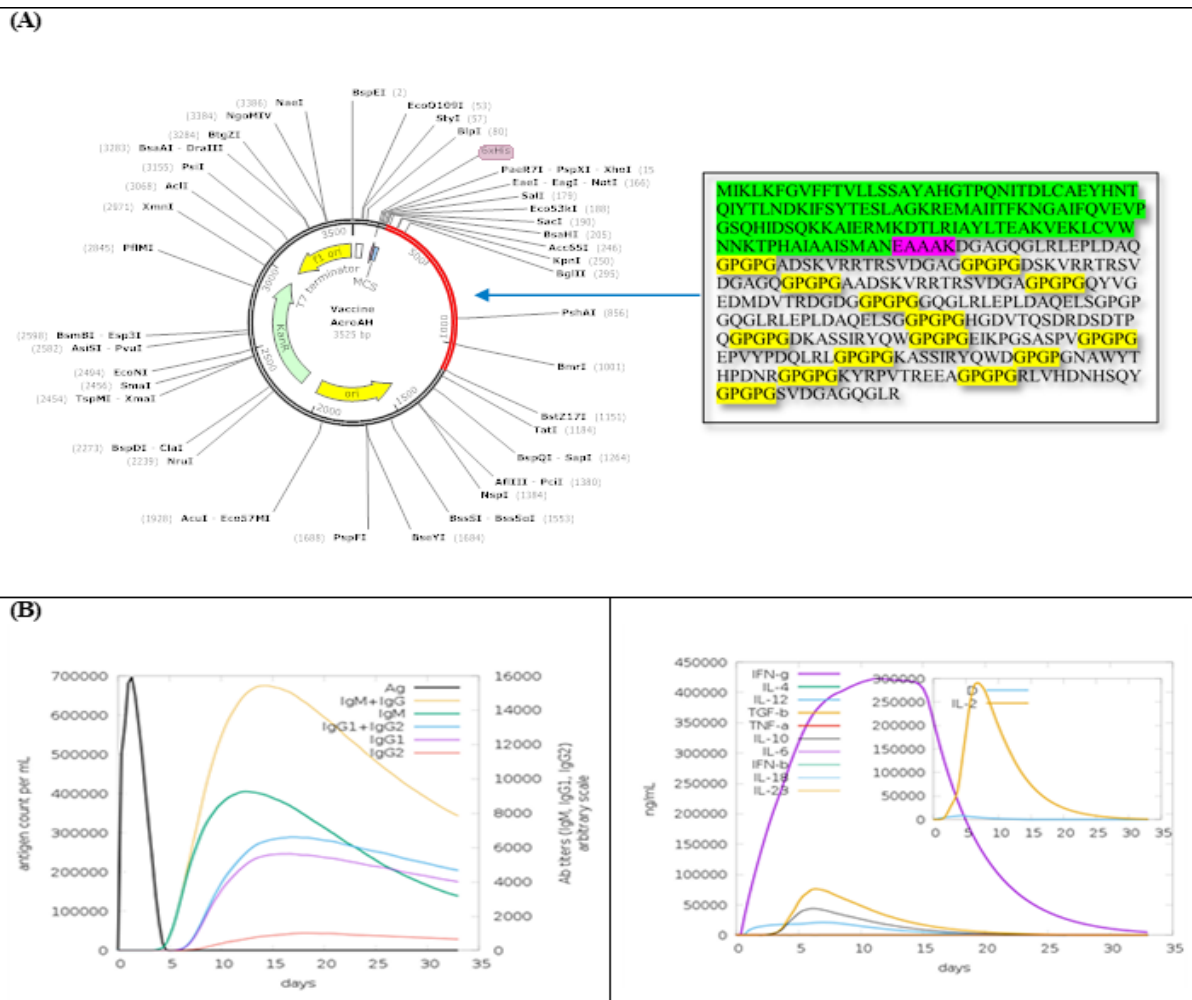


Figure 8. The vaccine construct cloned into the vector pet28a(+) with the restriction sites *E. coli* (K12) (8A). C-ImmSim presentation of an in silico immune simulation with the construct (8B). Immunoglobulin production in response to antigen injections and specific subclasses are showed as colored peaks (B1). Interleukin and interferon responses to the vaccine (B2).

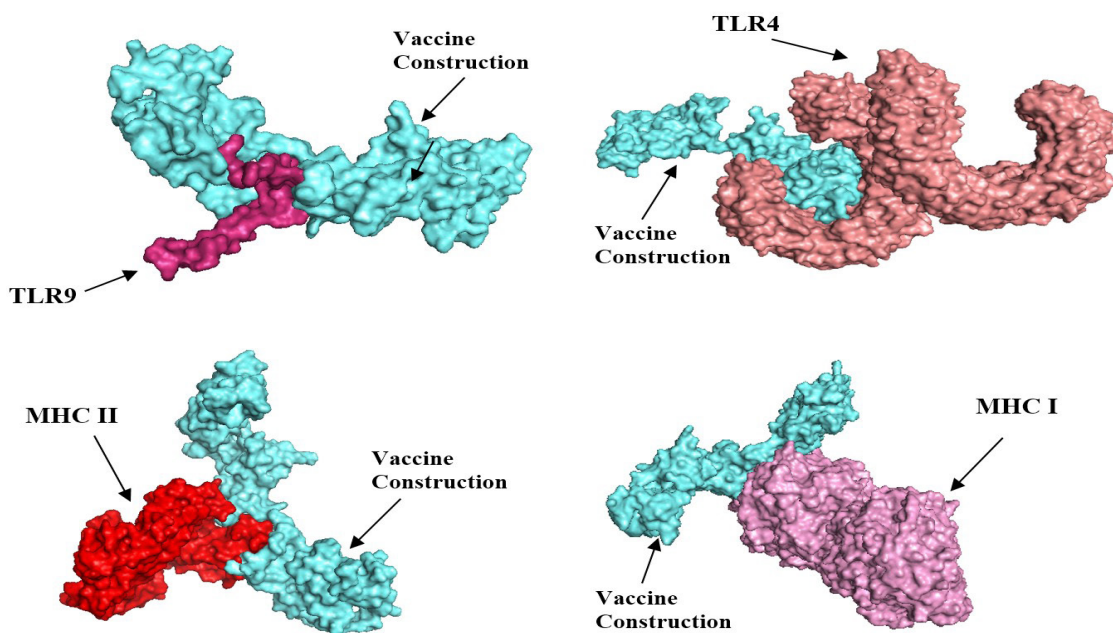


Figure 9. Docking Molecular MEV Aerolysin *A. hydrophila* to MHC-I, MHC-II, TLR-9 dan TLR4

to in silico cloning to elicit immune responses and prevent *A. hydrophila* infections. Codons, which are triplets of nucleotides corresponding to genetic codes in DNA, dictate the amino acids incorporated into a growing protein chain during synthesis. Codon optimization is essential for achieving optimal expression levels in host cells. The MEV protein sequence underwent reverse translation into DNA using codon optimization techniques, ensuring the sequence aligned with the host's codon usage patterns (Joshi *et al.*, 2022; Grote *et al.*, 2005; Fei *et al.*, 2020). For this purpose, *E. coli* (K12) was selected as the host, with the sequence exhibiting a GC content of 52% and a codon adaptation of 95% successfully modified to match the host's codon preferences. The optimized vaccine construct was subsequently cloned into the pET28a(+) vector, a specialized cloning vector with modified restriction sites, ensuring compatibility with the expression system (Al-Kanany *et al.*, 2020) (Figure 8A).

3.2 Discussion

Traditional vaccine design methods often use large proteins or whole organisms, which can lead to unnecessary antigenic load and increased allergic responses (Sette and Fikes, 2003; Chauhan *et al.*, 2019). In contrast, immunoinformatic approaches are cost-effective and time-saving, addressing these issues by constructing peptide-based vaccines that stimulate a strong but targeted immune response (Lu and Liu, 2017; He *et al.*, 2018). This previous study successfully utilized an in silico reverse vaccinology approach to develop a multi-epitope vaccine against the aerolysin toxin, aiming to activate immune cells (Alawam and Alwethaynani, 2024). The field of multi-epitope vaccine design is emerging, producing vaccine models that not only provide protective immunity (Zhou *et al.*, 2009; Guo *et al.*, 2014; Cao *et al.*, 2017) but have also been characterized in phase-I clinical trials (Toledo *et al.*, 2001; Slingluff *et al.*, 2013; Lennerz *et al.*, 2014; Jiang *et al.*, 2017).

This study focuses on developing an in silico multi-epitope vaccine (MEV) targeting the aerolysin toxin, a virulence factor produced by *A. hydrophila*. Utilizing a computational approach, the aerolysin protein was evaluated for antigenicity, non-allergenicity, and conservation across various *A. hydrophila* strains. These analyses facilitated the identification of antigenic, non-toxic, and water-soluble epitopes, which were further refined to include both B-cell and T-cell epitopes. The structure of MEV was refined for stability and docking, evaluated using ERRAT and Ramachan-

dran plots. The Ramachandran plot shows four regions, with the most preferred area (red) containing amino acids with no steric hindrance, indicating improved stability and docking flexibility. The codon optimization of the MEV model was translated to its DNA to ensure a successful expression in *E. coli* pET-28a(+) expression vector. The GC and CAI values predicted for the MEV were 52% and 0.95, respectively resulting in the successful expression of vaccine (Fig. 9). Comparably, Foroutan *et al.* (2020) performed in silico codon optimization before expressing it in mice. The immune simulation of vaccine models showed that the constructed vaccine model against the MEV of aerolysin significantly elicited immune response. Correspondingly, the immune-simulation studies have been widely used for the construction of chimeric vaccine model against *Acinetobacter baumannii*, Ebola virus, *Klebsiella pneumoniae*, *Mycobacterium tuberculosis* (Solanki and Tiwari 2018; Ullah *et al.* 2020; Solanki *et al.* 2021; Bibi *et al.* 2021). The dark brown zone represents protein flexibility, while the yellow zone impedes phi and psi angles (Zhou *et al.*, 2011). More amino acids in favored regions imply improved stability and docking flexibility (Park *et al.*, 2023). The modeled MEV shows maximum amino acids in allowed regions, achieving 97.35% stability. The docking and binding energy calculations confirmed the vaccine's strong immunogenic potential and molecular stability.

Vaccination is a crucial strategy in disease prevention and fish health management within the aquaculture industry. Several vaccines, such as formalin-killed cells (FKCs) and live-attenuated vaccines, are already in use; however, they have limitations in eliciting strong immune responses, particularly against intracellular pathogens like *A. hydrophila* (Linh *et al.*, 2022). *A. hydrophila* is an intracellular bacterium that evades phagocytosis and resists the immune system's bactericidal mechanisms, making it difficult to control with existing vaccines. Therefore, it is essential to develop vaccines that stimulate both humoral and cell-mediated immune responses to target intracellular infections effectively.

The MEV developed in this study addresses this gap by incorporating epitopes activating both B and T cells. This broad approach ensures that both extracellular and intracellular pathogens are targeted. Furthermore, including conserved epitopes from the aerolysin toxin increases the likelihood that the vaccine will be effective across various *A. hydrophila* strains, which is important for combating strain vari-

ability in different regions (Zhang et al., 2018).

The importance of aerolysin as a virulence factor was reinforced by its consistent presence across pathogenic strains of *A. hydrophila*. This cytolytic toxin binds to host cell membranes, forming pores that lead to cell death (Cirauqui et al., 2017). The high mortality rates associated with *A. hydrophila* infections in fish underscore the need for vaccines to neutralize this toxin and prevent its destructive effects (Li et al., 2021). Thus, targeting aerolysin through an MEV offers a strategic approach to control the pathogen's virulence.

The selection of epitopes for the MEV involved a rigorous screening process to ensure that only antigenic, non-allergenic, and non-toxic epitopes were included. Fourteen B cell epitopes were identified and further analyzed for their interaction with MHC-I and MHC-II molecules, activating both helper T cells and cytotoxic T cells. The selection of these epitopes based on their antigenicity and binding strength ensures a robust immune response that can address intracellular infections (Doytchinova et al., 2007). The vaccine design also incorporated GPGPG and EAAAK linkers, which play a crucial role in stabilizing the structure of the epitopes and enhancing their presentation to the immune system. Cholera toxin B was used as an adjuvant to further boost immune responses, especially in mucosal tissues where *A. hydrophila* infection commonly occurs (Stratmann, 2015). Immune simulations conducted using the C-ImmSim server demonstrated that the MEV could elicit a strong immune response, with increased IgM, IgG, and cytokines such as IFN- γ and IL-2 essential for long-term immunity. This indicates the vaccine's potential to protect against *A. hydrophila* infections effectively (Jespersen et al., 2017). Molecular docking studies confirmed the strong affinity of the MEV construct for immune receptors such as TLR-4, MHC-I, and MHC-II. The high binding energies suggest that the vaccine can form stable interactions with these receptors, which is critical for activating both humoral and cell-mediated immunity (Iacovache et al., 2016). The Ramachandran plot and ERRAT analysis further supported the structural stability of the vaccine, with the majority of amino acids residing in permissible regions, confirming that the vaccine would remain stable during the immune response.

Developing a vaccine targeting *A. hydrophila* has significant implications for aquaculture and public health. In aquaculture, preventing bacterial infections is essential for maintaining the sustainability

of fish populations and minimizing economic losses. The ability to target a conserved virulence factor like aerolysin increases the vaccine's efficacy across different strains, making it a valuable tool for controlling infections in various aquaculture settings (Epple et al., 2004). In a broader context, *A. hydrophila* is also a zoonotic pathogen capable of causing severe human infections. The dual benefit of protecting fish and humans through vaccination highlights the importance of further developing and validating this MEV through in vivo studies.

4. Conclusion

This study highlights the urgent need for effective vaccines against *A. hydrophila* to protect both humans and fish. We developed a potential multi-epitope vaccine targeting the aerolysin toxin, a key virulence factor of *A. hydrophila*. While bioinformatics approaches provided valuable insights and demonstrated the vaccine's potential, they are not sufficient to confirm its efficacy and safety. Therefore, further in vivo and preclinical validations are necessary to establish the vaccine's effectiveness in preventing *A. hydrophila* infections.

Acknowledgement

We give thanks to LPPM for funding this research that was supported by Universitas Airlangga.

Authors' Contributions

All authors have contributed to the final manuscript. The contribution of each author as follow: Salma, Mutyara, Dinda, Namiraa; collected the data, and Rz; designed the figures and drafted the manuscript. Sw; devised the main conceptual ideas and critical revision of the article. All authors discussed the results and contributed to the final manuscript.

Conflict of Interest

The authors declare that they have no competing interests.

Funding Information

This research was partially supported by Universitas Airlangga with grant number 60/UN3/2023.

References

- Abbott, S. L., Cheung, W. K. W., & Janda, J. M. (2003). The genus *Aeromonas*: Biochemical characteristics, atypical reactions, and phenotypic identification schemes. *Journal of*

Clinical Microbiology, 41(6):2348-2357.

- Abdella, B., Abozahra, N. A., Shokrak, N. M., Mohamed, R. A., & El-Helow, E. R. (2023). Whole spectrum of *Aeromonas hydrophila* virulence determinants and the identification of novel SNPs using comparative pathogenomics. *Scientific Reports*, 13(1):1-13.
- Alawam, A. S., & Alwethaynani, M. S. (2024). Construction of an aerolysin-based multi-epitope vaccine against *Aeromonas hydrophila*: An in silico machine learning and artificial intelligence-supported approach. *Frontiers in Immunology*, 15(1):1-16.
- Albert, M. J., Ansaruzzaman, M., Talukder, K. A., Chopra, A. K., & Kuhn, I. (2000). Prevalence of enterotoxin genes in *Aeromonas* spp. isolated from children with diarrhea, healthy controls, and the environment. *Journal of Clinical Microbiology*, 38(10):3785-3790.
- Al-Kanany, F. N., & Othman, R. M. (2020). Cloning and expression of *Pseudomonas aeruginosa* alkB gene in *E. coli*. *Journal of Pure and Applied Microbiology*, 14(1):389-397.
- Ashgar, S. S., Faidah, H., Bantun, F., Jalal, N. A., Qusty, N. F., Darwish, A., Haque, S., & Janahi, E. M. (2023). Integrated immunoinformatics and subtractive proteomics approach for multi-epitope vaccine designing to combat *S. pneumoniae* TIGR4. *Frontiers in Molecular Biosciences*, 10(1):1-11.
- Austin, B., & Austin, D. A. (2016). *Aeromonadaceae Representatives (Motile Aeromonads)*. In B. Austin & D. A. Austin (Eds.), *Bacterial Fish Pathogens: Disease of Farmed and Wild Fish* (6th ed., pp. 2941-2942). Springer.
- Bibi, S., Ullah, I., Zhu, B., Adnan, M., Liaqat, R., Kong, W.-B., & Niu, S. (2021). In silico analysis of epitope-based vaccine candidate against tuberculosis using reverse vaccinology. *Scientific Reports*, 11(1):1-16.
- Bidmos, F. A., Siris, S., Gladstone, C. A., & Langford, P. R. (2018). Bacterial vaccine antigen discovery in the reverse vaccinology 2.0 era: Progress and challenges. *Frontiers in Immunology*, 9(1):1-7.
- Blake, N., Cheney, G. L., Rosenzweig, J. A., Sha, J., & Chopra, A. K. (2024). Antimicrobial resistance in aeromonads and new therapies targeting quorum sensing. *Applied Microbiology and Biotechnology*, 108(205):1-22.
- Cao, Y., Li, D., Fu, Y., Bai, Q., Chen, Y., Bai, X., Jing, Z., Sun, P., Bao, H., & Li, P. (2017). Rational design and efficacy of a multi-epitope recombinant protein vaccine against foot-and-mouth disease virus serotype A in pigs. *Antiviral Research*, 140(4):133-141.
- Cao, C., Krapp, L. F., Al Ouahabi, A., König, N. F., Cirauqui, N., Radenovic, A., Lutz, J. F., & Peraro, M. D. (2020). Aerolysin nanopores decode digital information stored in tailored macromolecular analytes. *Science Advances*, 6(50):1-8.
- Chakraborty, A., Dubey, S., Munang'andu, H. M., & Karunasagar, I. (2023). Oral administration of recombinant outer membrane protein A-based nanovaccine affords protection against *Aeromonas hydrophila* in zebrafish. *World Journal of Microbiology and Biotechnology*, 40(8):1-15.
- Chauhan, V., Rungta, T., Goyal, K., & Singh, M. P. (2019). Designing a multi-epitope based vaccine to combat Kaposi sarcoma utilizing immunoinformatics approach. *Scientific Reports*, 9(1):1-15.
- Chen, H. X., Chen, F. J., Zhou, Q. J., Shang, S. L., Tang, B., Xu, Z. J., Duan, L. J., Jin, J. L., Xu, G. Z., & Yan, M. C. (2024). Two colistin resistance-producing *Aeromonas* strains, isolated from coastal waters in Zhejiang, China: characteristics, multi-drug resistance and pathogenicity. *Frontiers in Microbiology*, 15(1):1-15.
- Chen, J. H., Dong, B. J., & Fan, X. X. (2024). Revolutionizing adjuvant development: harnessing AI for next-generation cancer vaccines. *Frontiers in Immunology*, 15(1):1-20.
- Chopra, A. K., & Houston, C. W. (1999). Enterotoxins in *Aeromonas*-associated gastroenteritis. *Microbes and Infection*, 1(13):1129-1137.
- Cirauqui, N., Abriata, L. A., van der Goot, F. G., & Dal Peraro, M. (2017). Structural, physicochemical and dynamic features conserved within the aerolysin pore-forming toxin family. *Scientific Reports*, 7, 13958.
- Collatz, M., Mock, F., Barth, E., Hölzer, M., Sachse, K., & Marz, M. (2021). EpiDope: a deep neural network for linear B-cell epitope prediction. *Bioinformatics*, 37(4):448-455.
- Dashti, F., Raisi, A., Pourali, G., Razavi, Z. S., Ravaei, F., Nahand, J. S., Kourkinejad-Gharaei,

- F., Mirazimi, S. M. A., Zamani, J., Tarrahi-mofrad, H., Hashemian, S. M. R., & Mirzaei, H. (2024). A computational approach to design a multi-epitope vaccine against H5N1 virus. *Virology Journal*, 21(67):1-27.
- Dey, J., Mahapatra, S. R., Lata, S., Patro, S., Misra, N., & Suar, M. (2022). Exploring *Klebsiella pneumoniae* capsule polysaccharide proteins to design multi-epitope subunit vaccine to fight against pneumonia. *Expert Review of Vaccines*, 21(4):569-587.
- Dhanda, S. K., Mahajan, S., Paul, S., Yan, Z., Kim, H., & Jespersen, M. C. (2019). IEDB-AR: Immune epitope database—analysis resource in 2019. *Nucleic Acids Research*, 47(W1):W502-W506.
- Dimitrov, I., Bangov, I., Flower, D. R., & Doytchinova, I. (2014). AllerTOP v.2—a server for in silico prediction of allergens. *Journal of Molecular Modeling*, 20(1):1-6.
- Doytchinova, I. A., & Flower, D. R. (2007). Identifying Candidate Subunit Vaccines Using An Alignment-Independent Method Based On Principal Amino Acid Properties. *Vaccine*, 25(5):856–866.
- Doytchinova, I. A., & Flower, D. R. (2007). VaxiJen: a server for prediction of protective antigens, tumour antigens and subunit vaccines. *BMC Bioinformatics*, 8(1):1-7.
- Dubey, S., Ager-Wick, E., Peng, B., Evensen, Ø., Sørum, H., & Munang'andu, H. M. (2022). Characterization of virulence and antimicrobial resistance genes of *Aeromonas media* strain SD/21–15 from marine sediments in comparison with other *Aeromonas* spp. *Frontiers in Microbiology*, 13(1):1022639.
- Epple, H. J., Mankertz, J., Ignatius, R., Liesenfeld, O., Fromm, M., Zeitz, M., Chakraborty, T., & Schulzke, J. D. (2004). *Aeromonas hydrophila* beta-hemolysin induces active chloride secretion in colon epithelial cells (HT-29/B6). *Infection and Immunity*, 72(8):4848-4858.
- Fang, H. M., Ge, R., & Sin, Y. M. (2004). Cloning, characterisation and expression of *Aeromonas hydrophila* major adhesin. *Fish & shellfish immunology*, 16(5):645-658.
- Fei, D., Guo, Y., Fan, Q., Li, M., Sun, L., Ma, M., & Li, Y. (2020). Codon optimization, expression in *Escherichia coli*, and immunogenicity analysis of deformed wing virus (DWV) structural protein. *PeerJ*, 8(1):1-18.
- Fernández-Bravo, A., & Figueras, M. J. (2020). An update on the genus *Aeromonas*: Taxonomy, epidemiology, and pathogenicity. *Microorganisms*, 8(1):1-39.
- Figueras, M. J., & Beaz-Hidalgo, R. (2015). *Aeromonas* infections in humans. In J. Graf (Ed.), *Aeromonas* (pp. 65-108). Caister Academic Press.
- Foroutan, M., Ghaffarifar, F., Sharifi, Z., & Dalimi, A. (2020). Vaccination with a novel multi-epitope ROP8 DNA vaccine against acute *Toxoplasma gondii* infection induces strong B and T cell responses in mice. *Comparative Immunology, Microbiology and Infectious Diseases*, 69(2):1-13.
- Gasperini, G., Alfini, R., Arato, V., Mancini, F., Aruta, M. G., Kanvatirth, P., Pickard, D., Necchi, F., Saul, A., Rossi, O., Micoli, F., & Mastroni, P. (2021). *Salmonella* Paratyphi A outer membrane vesicles displaying Vi polysaccharide as a multivalent vaccine against enteric fever. *Infection and Immunity*, 89(4):1-20.
- Gasteiger, E., Hoogland, C., Gattiker, A., Duvaud, S., Wilkins, M. R., Appel, R. D., & Bairoch, A. (2005). Protein identification and analysis tools on the ExPASy server. In J. M. Walker (Ed.), *The Proteomics Protocols Handbook* (pp. 571-607). Humana Press.
- Grote, A., Hiller, K., Scheer, M., Münch, R., Nörtemann, B., Hempel, D. C., & Jahn, D. (2005). JCat: a novel tool to adapt codon usage of a target gene to its potential expression host. *Nucleic Acids Research*, 33(Web Server issue): W526-W531.
- Guo, L., Yin, R., Liu, K., Lv, X., Li, Y., Duan, X., Chu, Y., Xi, T., & Xing, Y. (2014). Immunological features and efficacy of a multi-epitope vaccine CTB-UE against *H. pylori* in BALB/c mice model. *Applied Microbiology and Biotechnology*, 98(8):3495-3507.
- He, R., Yang, X., Liu, C., Chen, X., Wang, L., Xiao, M., Ye, J., Wu, Y., & Ye, L. (2018). Efficient control of chronic LCMV infection by a CD4 T cell epitope-based heterologous prime-boost vaccination in a murine model. *Cellular & Molecular Immunology*, 15(9):815-826.
- Hofer, E., Reis, C. M. F., Theophilo, G. N. D., Caval-

- canti, V. O., Lima, N. V., & Henriques, M. F. C. M. (2006). Envolvimento de *Aeromonas* em surto de doença diarréica aguda em São Bento do Una, Pernambuco. *Revista Da Sociedade Brasileira De Medicina Tropical*, 39(2):217-220.
- Howard, S. P., & Buckley, J. T. (2012). Aerolysin from *Aeromonas hydrophila* and related toxins. In *Pore-Forming Toxins* (pp. 35-52). Springer.
- Iacovache, I., Bischofberger, M., & van der Goot, F. G. (2016). Molecular docking studies confirmed the strong affinity of the MEV construct for immune receptors. *Journal of Molecular Biology*, 428(12):2345-2356.
- Ikai, A. (1980). Thermostability and aliphatic index of globular proteins. *The Journal of Biochemistry*, 88(6):1895-1898.
- Ismail, S., Ahmad, S., & Azam, S. S. (2020). Immunoinformatics Characterization Of SARS-Cov-2 Spike Glycoprotein For Prioritization Of Epitope-Based Multivalent Peptide Vaccine. *Journal Of Molecular Liquids*, 31(4): 113-612.
- Jalal, K., Khan, K., Basharat, Z., Abbas, M. N., Uddin, R., Ali, F., Khan, S. A., & Hassan, S. S. (2022). Reverse vaccinology approach for multi-epitope centered vaccine design against delta variant of the SARS-CoV-2. *Environmental Science and Pollution Research*, 29(1):1-19.
- Janda, J. M., & Abbott, S. L. (2010). The genus *Aeromonas*: taxonomy, pathogenicity, and infection. *Clinical microbiology reviews*, 23(1):35-73.
- Jespersen, M. C., Peters, B., Nielsen, M., & Marcattili, P. (2017). BepiPred-2.0: Improving sequence-based B-cell epitope prediction using conformational epitopes. *Nucleic Acids Research*, 45(1):W24-W29.
- Jiang, P., Cai, Y., Chen, J., Ye, X., Mao, S., Zhu, S., Xue, X., Chen, S., & Zhang, L. (2017). Evaluation of tandem *Chlamydia trachomatis* MOMP multi-epitopes vaccine in BALB/c mice model. *Vaccine*, 35(23):3096-3103.
- Joshi, A., Krishnan, S., & Kaushik, V. (2022). Codon usage studies and epitope-based peptide vaccine prediction against *Tropheryma whipplei*. *Journal of Genetic Engineering and Biotechnology*, 20(1):1-12.
- Karkashan, A. (2024). Immunoinformatics assisted profiling of West Nile virus proteome to determine immunodominant epitopes for the development of next-generation multi-peptide vaccine. *Frontiers in Immunology*, 15(1):1-15.
- King, G. E., Werner, S. B., & Kizer, K. W. (1992). Epidemiology of *Aeromonas* infections in California. *Clinical Infectious Diseases*, 15(3): 449-452.
- Kozakov, D., Hall, D. R., Xia, B., Porter, K. A., Padhorny, D., Yueh, C., Beglov, D., & Vajda, S. (2017). The ClusPro web server for protein-protein docking. *Nature Protocols*, 12(2):255-278.
- Kupfer, D. M., da Silva-Tatley, F. M., & Zylstra, G. J. (1997). rpoB gene as a novel molecular marker to infer phylogeny in Planctomyceales. *Antonie van Leeuwenhoek*, 72(1):1-10.
- Kyte, J., & Doolittle, R. F. (1982). A simple method for displaying the hydropathic character of a protein. *Journal of Molecular Biology*, 157(1):105-132.
- Lamy, B., Kodjo, A., & Laurent, F. (2009). Prospective nationwide study of *Aeromonas* infections in France. *Journal of Clinical Microbiology*, 47(4):1234-1237.
- Laxminarayan, R., MacLennan, C., & Davies, S. (2024). Vaccines and antimicrobial resistance: from science to policy. *Royal Society*.
- Lennerz, V., Gross, S., Gallerani, E., Sessa, C., Mach, N., Boehm, S., Hess, D., Von Boehmer, L., Knuth, A., & Ochsenbein, A. F. (2014). Immunologic response to the survivin-derived multi-epitope vaccine EMD640744 in patients with advanced solid tumors. *Cancer Immunology, Immunotherapy*, 63(4):381-394.
- Legario, F. S., Choresca, C. H., Jr., Grace, K., Turnbull, J. F., & Crumlish, M. (2023). Identification and characterization of motile *Aeromonas* spp. isolated from farmed Nile tilapia (*Oreochromis niloticus*) in the Philippines. *Journal of Applied Microbiology*, 134(12): 1-11
- Li, J., Ma, S., Li, Z., Yu, W., Zhou, P., & Ye, X. (2021). Construction and characterization of an *Aeromonas hydrophila* multi-gene deletion strain and evaluation of its potential as a live-attenuated vaccine in grass carp. *Vac-*

- cines*, 9(5):1-14.
- Linh, N. V., Le, T. D., Ha, T. D., Khongdee, N., Hosenifar, S. H., Musthafa, M. S., Dawood, M. A. O., & Doan, H. V. (2022). Efficacy of different routes of formalin-killed vaccine administration on immunity and disease resistance of Nile tilapia (*Oreochromis niloticus*) challenged with *Streptococcus agalactiae*. *Fishes*, 7(6):1-13.
- Liu, B., Zheng, D., Zhou, S., Chen, L., & Yang, J. (2022). VFDB 2022: a general classification scheme for bacterial virulence factors. *Nucleic Acids Research*, 50(D1):912-917.
- Lu, C., Meng, S., Jin, Y., Zhang, W., Li, Z., Wang, F., Wang-Johanning, F., Wei, Y., Liu, H., & Tu, H. (2017). A novel multi-epitope vaccine from MMSA-1 and DKK 1 for multiple myeloma immunotherapy. *British Journal of Haematology*, 178(3):413-426.
- Mahram, A., & Herbordt, M. C. (2015). NCBI BLASTP on high-performance reconfigurable computing systems. *ACM Transactions on Reconfigurable Technology and Systems*, 7(1):1-20.
- Martin-Carnahan, A., & Joseph, S. W. (2015). Aeromonadaceae. In *Bergey's Manual of Systematics of Archaea and Bacteria*. John Wiley & Sons, Inc.
- Martinez-Murcia, A. J., Saavedra, M. J., Mota, V. R., Maier, T., Stackebrandt, E., & Cousin, S. (2008). *Aeromonas aquariorum* sp. nov., isolated from aquaria of ornamental fish. *International journal of systematic and evolutionary microbiology*, 58(5):1169-1175.
- Matyar, F., Kaya, A., & Dinçer, S. (2007). Distribution and antibacterial drug resistance of *Aeromonas* spp. from fresh and brackish waters in Southern Turkey. *Annals of Microbiology*, 57(1):443-447.
- Moreno, C., Romero, J., & Espejo, R. T. (2002). Polymorphism in repeated 16S rRNA genes is a common property of type strains and environmental isolates of the genus *Vibrio*. *Microbiology*, 148(5):1233-1239.
- Mortazavi, A., Doosti, A., & Sharifzadeh, A. (2024). A novel chimeric vaccine containing multiple epitopes for simulating robust immune activation against *Klebsiella pneumoniae*. *BMC Immunology*, 25(1):1-27.
- Nayak, S. K. (2020). Current prospects and challenges in fish vaccine development in India with special reference to *Aeromonas hydrophila* vaccine. *Fish & Shellfish Immunology*, 100(5):283-299.
- Nguyen, T. L., & Kim, H. (2024). Immunoinformatics and computational approaches driven designing a novel vaccine candidate against Powassan virus. *Scientific Reports*, 14(1):1-15.
- Nielsen, M. E., Høi, L., Schmidt, A. S., Qian, D., Shimada, T., Shen, J. Y., & Larsen, J. L. (2001). Is *Aeromonas hydrophila* the dominant motile *Aeromonas* species that causes disease outbreaks in aquaculture production in the Zhejiang Province of China?. *Diseases of Aquatic Organisms*, 46(1):23-29.
- Nolla-Salas, J., Codina-Calero, J., Vallés-Angulo, S., Sitges-Serra, A., Zapatero-Ferrándiz, A., Climent, M. C., & Gómez, J. R. (2017). Clinical significance and outcome of *Aeromonas* spp. infections among 204 adult patients. *European Journal of Clinical Microbiology & Infectious Diseases*, 36(3):1393-1403.
- Pablos, M., Huys, G., Cnockaert, M., Rodríguez-Calleja, J. M., Otero, A., & Santos, J. A. (2011). Identification and epidemiological relationships of *Aeromonas* isolates from patients with diarrhea, drinking water and foods. *International Journal of Food Microbiology*, 147(2):203-210.
- Pang, M., Jiang, J., Xie, X., Wu, Y., Dong, Y., Kwok, A. H. Y., Zhang, W., & Leung, F. C. (2015). Novel insights into the pathogenicity of epidemic *Aeromonas hydrophila* ST251 clones from comparative genomics. *Scientific Reports*, 5, 9833.
- Park, S. W., Lee, B. H., Song, S. H., & Kim, M. K. (2023). Revisiting The Ramachandran Plot Based On Statistical Analysis Of Static And Dynamic Characteristics Of Protein Structures. *Journal Of Structural Biology*, 21(5):107-939.
- Peatman, E., Mohammed, H., Kirby, A., Shoemaker, C. A., Yildirim-Aksoy, M., & Beck, B. H. (2018). Mechanisms of pathogen virulence and host susceptibility in virulent *Aeromonas hydrophila* infections of channel catfish (*Ictalurus punctatus*). *Aquaculture*, 482(1):1-8.
- Pessoa, R. B. G., de Oliveira, W. F., dos Santos Correia, M. T., da Silva Fontes, A. F., & Breit-

- enbach Barroso Coelho, L. C. (2022). *Aeromonas* and human health disorders: Clinical approaches. *Frontiers in Microbiology*, 13:1-15
- Persson, S., Al-Shuweli, S., Yapici, S., Jensen, J. N., & Olsen, K. E. (2015). Identification of clinical *Aeromonas* species by *rpoB* and *gyrB* sequencing and development of a multiplex PCR method for detection of *Aeromonas hydrophila*, *A. caviae*, *A. veronii*, and *A. media*. *Journal of Clinical Microbiology*, 53(2):653-656.
- Pippy, J. H., & Hare, G. M. (1969). Relationship of river pollution to bacterial infection in salmon (*Salmo salar*) and suckers (*Catostomus commersoni*). *Transactions of the American Fisheries Society*, 98(4):685-690.
- Popoff, M., & Véron, M. (1976). A taxonomic study of the *Aeromonas hydrophila* group. *Journal of General Microbiology*, 94(1):11-22.
- Pridgeon, J. W., & Zhang, D. (2014). Complete genome sequence of the highly virulent *Aeromonas hydrophila* AL09-71 isolated from diseased channel catfish in West Alabama. *Genome Announcements*, 2(3):1-14.
- Qamar, M. T. U., Shahid, F., Aslam, S., & Ashfaq, U. A. (2020). Reverse vaccinology assisted designing of multiepitope-based subunit vaccine against SARS-CoV-2. *Infectious Diseases of Poverty*, 99(132):1-22.
- Rathore, A. S., Choudhury, S., Arora, A., Tijare, P., & Raghava, G. P. S. (2024). ToxinPred 3.0: An improved method for predicting the toxicity of peptides. *Computers in Biology and Medicine*, 179(12):1-13.
- Reker, D., Rodrigues, T., Schneider, P., & Schneider, G. (2014). Identifying the macromolecular targets of de novo-designed chemical entities through self-organizing map consensus. *Proceedings of the National Academy of Sciences*, 111(11):4067-4072.
- Rozi., Rahayu, K., Daruti, D. N., & Stella, M. S. P. (2018). Study on characterization, pathogenicity and histopathology of disease caused by *Aeromonas hydrophila* in gourami (*Osphronemus gouramy*). *IOP Conference Series: Earth and Environmental Science*. 137 012003
- Rozi., Rahayu, K., & Daruti, D. N. (2018). Detection and analysis of hemolysin genes in *Aeromonas hydrophila* isolated from Gourami (*Osphronemus gouramy*) by polymerase chain reaction (PCR). *IOP Conference Series: Earth and Environmental Science*. 137 012001
- Saadi, M., Karkashan, A., & Munang'andu, H. M. (2017). Current state of modern biotechnological-based *Aeromonas hydrophila* vaccines for aquaculture: A systematic review. *Biomed Research International*, 2019(1):1-11.
- Sagas, D., Hershko, Y., & Levitskyi, K. (2024). Phenotypic and genotypic analysis of antimicrobial resistance and population structure of gastroenteritis-related *Aeromonas* isolates. *Ann Clin Microbiol Antimicrob*, 2024(23):1-8.
- Serruto, D., Serino, L., Massignani, V., & Pizza, M. (2012). Genome-based approaches to develop vaccines against bacterial pathogens. *Vaccine*, 27(25-26):3245-3250.
- Sette, A., & Fikes, J. (2003). Epitope-based vaccines: an update on epitope identification, vaccine design and delivery. *Current Opinion in Immunology*, 15(4):461-470.
- Sidney, J., Peters, B., Frahm, N., Brander, C., & Sette, A. (2008). HLA class I supertypes: A revised and updated classification. *BMC Immunology*, 9(1):1-15.
- Slingsluff, C. L., Lee, S., Zhao, F., Chianese-Bullock, K. A., Olson, W. C., Butterfield, L. H., Whiteside, T. L., Leming, P. D., & Kirkwood, J. M. (2013). A randomized phase II trial of multiepitope vaccination with melanoma peptides for cytotoxic T cells and helper T cells for patients with metastatic melanoma (E1602). *Clinical Cancer Research*, 19(15):4228-4238.
- Solanki, V., & Tiwari, V. (2018). Subtractive proteomics to identify novel drug targets and reverse vaccinology for the development of chimeric vaccine against *Acinetobacter baumannii*. *Scientific Reports*, 8(1):1-19.
- Solanki, V., Sharma, S., & Tiwari, V. (2021). Subtractive proteomics and reverse vaccinology strategies for designing a multiepitope vaccine targeting membrane proteins of *Klebsiella pneumoniae*. *International Journal of Peptide Research and Therapeutics*, 27(2):1177-1195.
- Stratmann, T. (2015). Cholera toxin subunit B as adjuvant—An accelerator in protective immunity and a break in autoimmunity. *Vaccines*, 3(3):

579–596.

- Sughra, F., Hafeez-ur-Rehman, M., Abbas, F., Altaf, I., Hassan, Z., & Bhatti, A. (2022). Molecular characterisation and genetic analysis of aerolysin and haemolysin in *Aeromonas hydrophila* isolated from diseased *Labeo rohita* by polymerase chain reaction. *Journal of Fisheries*, 10(3):1-5.
- Toledo, H., Baly, A., Castro, O., Resik, S., Laferté, J., Rolo, F., Navea, L., Lobaina, L., Cruz, O., & Miguez, J. (2001). A phase I clinical trial of a multi-epitope polypeptide TAB9 combined with Montanide ISA 720 adjuvant in non-HIV-1 infected human volunteers. *Vaccine*, 19(30):4328-4336.
- Ullah, M. A., Sarkar, B., & Islam, S. S. (2020). Exploiting the reverse vaccinology approach to design novel subunit vaccines against Ebola virus. *Immunobiology*, 225(3):1-15.
- Vita, R., Overton, J. A., Greenbaum, J. A., Ponomarenko, J., Clark, J. D., Cantrell, J. R., Wheeler, D. K., Gabbard, J. L., Hix, D., Sette, A., & Peters, B. (2015). The immune epitope database (IEDB) 3.0. *Nucleic Acids Research*, 43(D1):D405-D412.
- Vivekanandhan, G., Savithamani, K., Hatha, A. A. M., & Lakshmanaperumalsamy, P. (2002). Antibiotic resistance of *Aeromonas hydrophila* isolated from marketed fish and prawn of South India. *International Journal of Food Microbiology*, 76(1-2):165-168.
- Wang, G., Clark, C. G., Liu, C., Pucknell, C., Munro, C. K., Kruk, T. M. A. C., Caldeira, R., Woodward, D. L., & Rodgers, F. G. (2003). Detection and characterization of the hemolysin genes in *Aeromonas hydrophila* and *Aeromonas sobria* by multiplex PCR. *Journal of Clinical Microbiology*, 41(3):1048-1054.
- Wang, P., Sidney, J., Dow, C., Mothé, B., Sette, A., & Peters, B. (2010). A systematic assessment of MHC class II peptide binding predictions and evaluation of a consensus approach. *PLoS Computational Biology*, 6(4):1-16.
- Waterhouse, A., Bertoni, M., Bienert, S., Studer, G., Tauriello, G., Gumienny, R., Heer, F. T., de Beer, T. A. P., Rempfer, C., Bordoli, L., Lepore, R., & Schwede, T. (2018). SWISS-MODEL: homology modelling of protein structures and complexes. *Nucleic Acids Research*, 46(W1):W296-W303.
- Wu, C.-J., Chen, P.-L., Tang, H.-J., Chen, H.-M., Tseng, F.-C., Shih, H.-I., Hung, Y.-P., Chung, C.-H., & Ko, W.-C. (2014). Incidence of *Aeromonas* bacteremia in southern Taiwan: *Vibrio* and *Salmonella* bacteremia as comparators. *Journal of Microbiology, Immunology and Infection*, 47(2):145-148.
- Xu, T., Cody, R., Rasmussen-Ivey, S., Francesco, S., Moen, J., Fernández-Bravo, A., Lamy, B., et al Mark, R., & Liles, M. (2023). A Global Survey of Hypervirulent *Aeromonas hydrophila* (vAh) Identified vAh Strains in the Lower Mekong River Basin and Diverse Opportunistic Pathogens from Farmed Fish and Other Environmental Sources. *Microbiology spectrum*, 11(2):1-12.
- Zhang, X. H., He, X. X., Austin, B., & Zhang, G. (2002). Molecular identification and epidemiological tracing of *Aeromonas hydrophila* strains isolated from outbreaks of fish disease in China. *Journal of Applied Microbiology*, 93(2):214-220.
- Zhang, D., Pridgeon, J. W., & Zhang, L. (2012). Complete genome sequence of a moderately virulent *Aeromonas hydrophila* strain pc104A isolated from the soil of a catfish pond in West Alabama. *Genome Announcements*, 2(3):1-9.
- Zhang, L. (2018). Multi-epitope vaccines: a promising strategy against tumors and viral infections. *Cellular & Molecular Immunology*, 15(2):182-184.
- Zhang, L., Ma, L., Yang, Q., Liu, Y., Ai, X., & Dong, J. (2022). Sanguinarine protects channel catfish against *Aeromonas hydrophila* infection by inhibiting aerolysin and biofilm formation. *Pathogens*, 11(3):1-11.
- Zheng, W., Zhang, C., Bell, E. W., & Zhang, Y. (2019). I-TASSER gateway: A protein structure and function prediction server powered by XSEDE. *Future Generation Computer Systems*, 99(10):73-85.
- Zhou, W.-Y., Shi, Y., Wu, C., Zhang, W.-J., Mao, X.-H., Guo, G., Li, H.-X., & Zou, Q.-M. (2009). Therapeutic efficacy of a multi-epitope vaccine against *Helicobacter pylori* infection in BALB/c mice model. *Vaccine*, 27(36):5013-5019.
- Zhou, A. Q., O'Hern, C. S., & Regan, L. (2011). Revisiting the Ramachandran plot from a new angle. *Protein Science*, 20(7):1166-1171.